doi:10.5598/imafungus.2017.08.02.02

IMA FUNGUS · 8(2): 219–244 (2017)

ARTICLE

Multiple new cryptic pathogenic *Phytophthora* species from *Fagaceae* forests in Austria, Italy and Portugal

Thomas Jung[1,2,3], Marília Horta Jung[1,2,3], Santa Olga Cacciola[4], Thomas Cech[5], József Bakonyi[6], Diána Seress[6], Saveria Mosca[7], Leonardo Schena[7], Salvatore Seddaiu[8], Antonella Pane[4], Gaetano Magnano di San Lio[7], Cristiana Maia[2], Alfredo Cravador[2], Antonio Franceschini[9], and Bruno Scanu[9]

[1]Phytophthora Research Centre, Mendel University, 613 00 Brno, Czech Republic
[2]Laboratory of Molecular Biotechnology and Phytopathology, Centre for Mediterranean Bioresources and Food, University of Algarve, 8005–130 Faro, Portugal
[3]Phytophthora Research and Consultancy, 83131 Nußdorf, Germany
[4]Department of Agriculture, Food and Environment, University of Catania, 95123 Catania, Italy
[5]Federal Research and Training Centre for Forests, Natural Hazards and Landscape (BFW), Seckendorff-Gudent-Weg 8, A-1131 Vienna, Austria
[6]Plant Protection Institute, Centre for Agricultural Research, Hungarian Academy of Sciences, Budapest, Hungary
[7]Dipartimento di Agraria, University Mediterranea of Reggio Calabria, 89122 Reggio Calabria, Italy
[8]Dipartimento della ricerca per il sughero e la silvicoltura, Agris Sardegna, Via Limbara 9, 07029 Tempio Pausania, Italy
[9]Dipartimento di Agraria, Sezione di Patologia vegetale ed Entomologia, Università degli Studi di Sassari, Viale Italia 39, 07100 Sassari, Italy; corresponding author e-mail: bscanu@uniss.it

Abstract: During surveys of *Phytophthora* diversity in natural and semi-natural *Fagaceae* forests in Austria, Italy and Portugal, four new cryptic species were isolated from rhizosphere soil samples. Multigene phylogeny based on nuclear ITS, ß-tubulin and HSP90 and mitochondrial *cox*1 and NADH1 gene sequences demonstrated that two species, *P. tyrrhenica* and *P. vulcanica* spp. nov., belong to phylogenetic Clade 7a, while the other two species, *P. castanetorum* and *P. tubulina* spp. nov., clustered together with *P. quercina* forming a new clade, named here as Clade 12. All four new species are homothallic and have low optimum and maximum temperatures for growth and very slow growth rates at their respective optimum temperature. They differed from each other and from related species by a unique combination of morphological characters, cardinal temperatures, and growth rates. Pathogenicity of all *Phytophthora* species to the root system of their respective host species was demonstrated in soil infestation trials.

Key words:
Clade 7
cryptic species
evolution
homothallic
phylogeny
Phytophthora quercina
species radiation

Article info: Submitted: 11 May 2017; Accepted: 20 September 2017; Published: 28 September 2017.

INTRODUCTION

The family *Fagaceae* comprises about 1000 species belonging to eight to ten genera widely distributed across the Northern Hemisphere (Manos & Stanford 2001). In Europe, species from the genera *Castanea*, *Fagus*, and *Quercus* dominate a wide variety of habitats ranging from Mediterranean sclerophyllous evergreen communities to temperate, deciduous lowland and mountainous forests (http://www.euforgen.org). Besides species with wide geographical distributions and ecological amplitudes, such as sweet chestnut (*Castanea sativa*) and European beech (*Fagus sylvatica*), some evergreen oaks (e.g. *Quercus ilex* and *Q. suber*) are geographically restricted and adapted to particular environmental conditions such as prolonged summer drought and fire (Schirone *et al.* 2016). Although species in these genera constitute primarily forest resources important for their wide range of uses (biomass, fibre, wood products, cork and food), they are also keystone species in forest ecosystems and considered main drivers of terrestrial biodiversity (Kremer *et al.* 2012). In some countries, they are major patrimonial and cultural resources (Logan 2005).

Since the early 1990s, numerous surveys in declining and healthy European *Fagaceae* forests have revealed a wealth of resident *Phytophthora* species (Jung 2009, Perez-Sierra *et al.* 2013, Scanu *et al*. 2013). Several *Phytophthora* species, including *P. cactorum*, *P.* x*cambivora* (previously known as *P. cambivora*), *P. cinnamomi*, *P. plurivora,* and *P. quercina* were strongly associated with the decline and dieback of forests, while other species, such as *P. cryptogea*, *P. europaea*, *P. gallica*, *P. gonapodyides*, *P. megasperma*, *P. pseudosyringae*, *P. psychrophila*, *P. syringae*, *P. uliginosa*, *P.* sp. forestsoil, and *P.* sp. riversoil, were more cryptic, and their role in forest ecosystems is still not fully understood.

Between 2010 and 2016, surveys of *Phytophthora* diversity were independently performed in forests in Austria, Italy, and Portugal during which four new cryptic *Phytophthora* species were recovered from the rhizosphere of *Fagaceae*

species. All four species showed scattered distribution, very slow growth in culture, and were difficult to isolate using traditional soil baiting methods. Preliminary analysis of sequence data from the ITS region of the nrDNA and part of the mitochondrial *cox*1 gene showed that two taxa were closely related to *P. uliginosa* from subclade a of phylogenetic Clade 7 (in the following Clade 7a) whereas the other two taxa clustered with *P. quercina* and the informally designated taxon *Phytophthora* sp. ohioensis.

In this study, morphological and physiological characteristics are used in combination with DNA sequence data from the ITS, part of the nuclear heat shock protein 90 (HSP90) and β-tubulin (Btub), and the mitochondrial *cox*1 and NADH1 genes to characterize the four putative new *Phytophthora* taxa isolated from *Fagaceae* forests in Austria, Italy, and Portugal, and compare them to their closest relatives. The results of this study are presented and the new taxa described as *P. castanetorum, P. tyrrhenica*, *P. tubulina*, and *P. vulcanica* spp. nov. Pathogenicity of all new *Phytophthora* species against their respective hosts was also tested in soil infestation trials to confirm Koch's postulates.

MATERIAL AND METHODS

Phytophthora isolation and culture maintenance

Isolates were obtained from rhizosphere soil of mature trees (Supplementary Table 1) using the sampling and isolation methods described by Jung *et al.* (1996), Jung (2009), and Scanu *et al.* (2015). Additional isolates used in the phylogenetic, morphological, and physiological studies and in the pathogenicity tests were sourced from the culture collections of the authors (Supplementary Table 1). In addition, isolates of *P. quercina* were obtained between 2010 and 2014 from various *Quercus* species in Portugal and Poland for comparative studies (Supplementary Table 1). For all isolates, single hyphal tip cultures were produced under the stereomicroscope from the margins of fresh cultures on V8-juice agar (V8A; 16 g agar, 3 g CaCO3, 100 mL Campbell's V8 juice, 900 mL distilled water). Stock cultures were maintained on carrot agar (CA; 16 g agar, 3 g CaCO3, 200 g carrot, 1000 mL distilled water; Scanu *et al.* 2014a) at 10 °C in the dark. All isolates of the four new species are preserved in the culture collections maintained at Mendel University (BD numbers, referring to the BioDiversA project RESIPATH), the University of Sassari (P and PH numbers, both referring to *Phytophthora*) and the University of Catania (Roman numbers). Dried culture holotypes were lodged with the CBS Herbarium, and ex-type and isotype cultures were deposited at the Westerdijk Fungal Biodiversity Institute (CBS; Utrecht, The Netherlands) (Supplementary Table 1).

DNA isolation, amplification and sequencing

Extraction of mycelial DNA was performed according to Jung *et al.* (2017b) using the DNeasy Plant Mini kit (QIAGEN, Hilden) or the E.Z.N.A.® Fungal DNA Mini Kit (OMEGA Biotek, Norcross, GA) following the manufacturer's instructions and checked for quality and quantity by spectrophotometry. DNA was stored at –20 °C until required. For 29 isolates of the four new *Phytophthora* species and five isolates of *P. quercina*, three nuclear and two mitochondrial loci were amplified and sequenced (Supplementary Table 1). The ITS1-5.8S-ITS2 region of the nrDNA was amplified using the primer-pair ITS1/ITS4 (White *et al.* 1990) and the PCR reaction mixture and cycling conditions described by Nagy *et al.* (2003) with an annealing temperature of 57 °C for 30 s. Partial heat shock protein 90 (HSP90) gene was amplified with the primer-pair HSP90F1int/HSP90R1 as described previously (Blair *et al.* 2008). Segments of the β-tubulin (Btub) and the mitochondrial genes cytochrome c oxidase subunit 1 (*cox*1) and NADH dehydrogenase subunit 1 (NADH1) were amplified using primer-pairs TUBUF2/TUBUR1, COXF4N/COXR4N and NADHF1/NADHR1, respectively, and the PCR reaction mixture and cycling conditions as described by Kroon *et al.* (2004). Products of Thermo Fisher Scientific (Waltham, MA) and Bio-Rad C1000™ or Applied Biosystems® 2720 Thermal Cyclers were used for the PCR reactions. Amplicons were purified and sequenced in both directions using the primers of the PCR reactions by Macrogen Inc. (Amsterdam) and BMR Genomics DNA sequencing service (www.bmrgenomics.it).

Electrophoregrams were quality checked and forward and reverse reads were compiled using Pregap4 version 1.5 and Gap v.4.10 of the Staden software package (Staden *et al.* 2000). Heterozygous sites were labelled according to the IUPAC coding system. All sequences derived in this study were deposited in GenBank and accession numbers are given in Supplementary Table 1.

Phylogenetic analysis

DNA sequences generated were combined with sequences of *Phytophthora* species obtained from GenBank. Sequences of each locus were aligned using the online MAFFT version 7 (http://mafft.cbrc.jp/alignment/server/) (Katoh & Standley 2013) by the E–INS–I strategy (ITS) or the G-INS-i option (all other loci). The phylogenetic analyses of *P. tyrrhenica* and *P. vulcanica* from Clade 7a, and of *P. castanetorum* and *P. tubulina* from the *P. quercina* clade were performed separately.

For the phylogenetic analyses of *P. tyrrhenica* and *P. vulcanica* all 16 previously known taxa from Clade 7a were included and *P. cinnamomi* (CBS 144.22) and *P. niederhauserii* (CBS 124086), both from Clade 7b, were used as outgroups (Abad *et al.* 2014, Jung *et al*. 2017b). The datasets of the five loci were first analysed separately and then combined. The 5-loci dataset comprised 4257 characters (ITS=842, Btub=911, HSP90=840, *cox*1=867, NADH1=797) and included 43 *Phytophthora* isolates.

To resolve the phylogenetic positions of *P. castanetorum* and *P. tubulina* within the *P. quercina* clade, and of the latter within the genus *Phytophthora*, 24 isolates from seven putative taxa of the *P. quercina* clade, including *P. castanetorum*, *P. tubulina*, *P. quercina*, *P. versiformis* (Paap *et al.* 2017), and the undescribed taxa *P.* sp. ohioensis, *P.* sp. quercina-like (only ITS sequence available), and *P.* sp. versiformis-like, and representative species from all phylogenetic *Phytophthora* clades were included in the analyses. The designated ex-type isolate (CBS 142348) of *Nothophytophthora amphigynosa*, the type species of a new sister genus of *Phytophthora* (Jung *et al.* 2017c) was

used as outgroup taxon in all analyses. The datasets of the five loci were first analysed separately and then combined. The *cox*1 sequences of *P.* sp. ohioensis, *P. versiformis* and *P.* sp. versiformis-like from GenBank were generated using primer pair FM77/FM84 (Martin & Tooley 2003) and, hence, had insufficient overlap with those of *P. castanetorum*, *P. quercina* and *P. tubulina* generated in this study with primer pair COXF4N/COXR4N. Therefore, *cox*1 was excluded from the two multigene analyses of the *P. quercina* clade. The combined four locus dataset comprised 3539 characters (ITS=992, Btub=915, HSP90=843, NADH1=789). For 11 of the 24 *Phytophthora* species from other clades no isolates with sequences for all four loci were available at GenBank or at Phytophthora database, hence sequences from two different isolates per species were combined (Supplementary Table 1). Since for *P. lilii* no NADH1 sequence was available a separate analysis of a combined nuclear ITS-Btub-HSP90 dataset was performed in order to clarify whether *P. lilii* constitutes a distinct phylogenetic clade as suggested by Rahman *et al.* (2015) and whether the inclusion of *P. lilii* has any effect on the grouping of the *P. quercina* clade. This three locus dataset comprised 2768 characters (ITS=1010, Btub=915, HSP90=843) and included 49 *Phytophthora* taxa.

For all individual gene and all multigene alignments, both Maximum Lkelihood (ML) phylogenetic and Bayesian Inference (BI) analyses were performed. ML analyses of the datasets were carried out with RAxML (Stamatakis 2014) in the raxmlGUI version 1.5b1 (Silvestro & Michalak 2012) implemented with the GTRGAMMA model. There were 10 runs of the ML and bootstrap ("thorough boostrap") analyses with 1000 replicates used to test the support of the branches. Phylogenetic BI analyses were performed with MrBayes 3.1.2 (Huelsenbeck & Ronquist 2001, Ronquist & Huelsenbeck 2003) using the GTR+G model. For multigene BI analyses the individual gene alignments were divided into five (Clade 7a) and four or three (*P. quercina* clade) partitions, respectively. Four Markov chains were run for 10 million generations with three heated chains (temperature = 0.2) and one cold chain. Trees were sampled every 1000 steps after removing the first 6000 generations as burn in. For the multigene BI analysis of Clade 7a 20 million, generations with a burn in of the first 8000 generations were used. Phylogenetic trees were visualized in MEGA6 (Tamura *et al.* 2013) and edited in figure editor programs. All alignments and trees deriving from BI and ML analyses were deposited in TreeBASE (20982; http://purl.org/phylo/treebase/phylows/study/TB2:S20982).

Morphology of asexual and sexual structures

Morphological features and morphometric data of sporangia, oogonia, oospores, antheridia, chlamydospores, hyphal swellings, and aggregations of the four new species were compared with each other and with those of related species from published studies.

Formation of sporangia was induced by submerging two 12–15 mm square discs cut from the growing edge of a 3-7-d-old V8A colony in a 90 mm diam Petri dish in non-sterile soil extract (50 g of filtered oak forest soil in 1000 mL of distilled water, filtered after 24 h; Jung *et al.* 1996). The Petri dishes were incubated at 20 ºC in natural daylight and the soil extract changed after ca 6 h (Jung *et al.* 2017b). Shape, type of apex, caducity and special features of sporangia and the formation of hyphal swellings and aggregations were recorded after 24–48 h. For each isolate 50 sporangia were measured at x400 using a compound microscope (Zeiss Imager.Z2), a digital camera (Zeiss Axiocam ICc3) and a biometric software (Zeiss AxioVision).

The formation of gametangia (oogonia and antheridia) and their characteristic features were examined on V8A after 21-30 d growth at 20 ºC in the dark. For each isolate each 50 oogonia, oospores and antheridia chosen at random were measured under a compound microscope at x400 as described before. The oospore wall index was calculated according to Dick (1990).

For comparisons, morphometric, morphological and physiological data of *P. quercina* and *Phytophthora* species from Clade 7a, respectively, were taken from published descriptions (Jung *et al.* 1999, 2002, 2017b).

Colony morphology, growth rates and cardinal temperatures

Colony growth patterns of *Phytophthora* species were described from 15-d-old (Clade 7a species) and 10-d-old (*P. castanetorum*, *P. quercina,* and *P. tubulina*) cultures grown at 20 °C in the dark on CA, V8A, malt-extract agar (MEA; Oxoid, Basingstoke, UK) and potato-dextrose agar (PDA; Oxoid) according to Scanu *et al*. (2014a), Jung *et al.* (1999, 2017b), and Erwin & Ribeiro (1996).

For temperature-growth relationships, representative isolates of the four new *Phytophthora* species and *P. quercina* (Supplementary Table 1) were subcultured onto 90 mm V8A plates and incubated for 24 h at 20 °C to stimulate onset of growth (Jung *et al.* 1999). Then, three replicate plates per isolate were transferred to 5, 10, 15, 20, 25, 30, and 35 °C. Radial growth was recorded after 6 d, along two lines intersecting the centre of the inoculum at right angles and the mean growth rates (mm/d) were calculated. Plates showing no growth at 30 or 35 °C were returned to 20 °C to determine isolate viability.

Soil infestation trials

In order to fulfil Koch's postulates, pathogenicity of all four new *Phytophthora* species was tested using the soil infestation method described by Jung *et al.* (1996). *Phytophthora tubulina* and *P. vulcanica* were tested in trial 1 with 3-year-old saplings of *Fagus sylvatica*, while *P. castanetorum* and *P. tyrrhenica* were tested in trial 2 with 1-year-old seedlings of *Castanea sativa*, and *Quercus ilex* and *Q. suber*, respectively. Saplings and seedlings were sourced from local nurseries and confirmed to be non-infested by *Phytophthora* using the soil baiting method described before. Two isolates for each new *Phytophthora* species were used, and isolates of *P.* x*cambivora* and *P. cinnamomi* (both primary pathogens of *Fagaceae*) were included as positive controls (Supplementary Table 1). Inocula consisted of 4-wk-old cultures of the respective *Phytophthora* isolate grown at 20 ºC in 500 mL Erlenmeyer flasks on an autoclaved mixture of 250 cm3 of vermiculite and 20 cm3 of millet seeds thoroughly moistened with 175 mL of V8-juice broth (200 mL/L juice, 800 mL/L distilled water amended with 3 g/L CaCO3) (Jung *et al.* 1996). Before use, the colonized medium was rinsed with

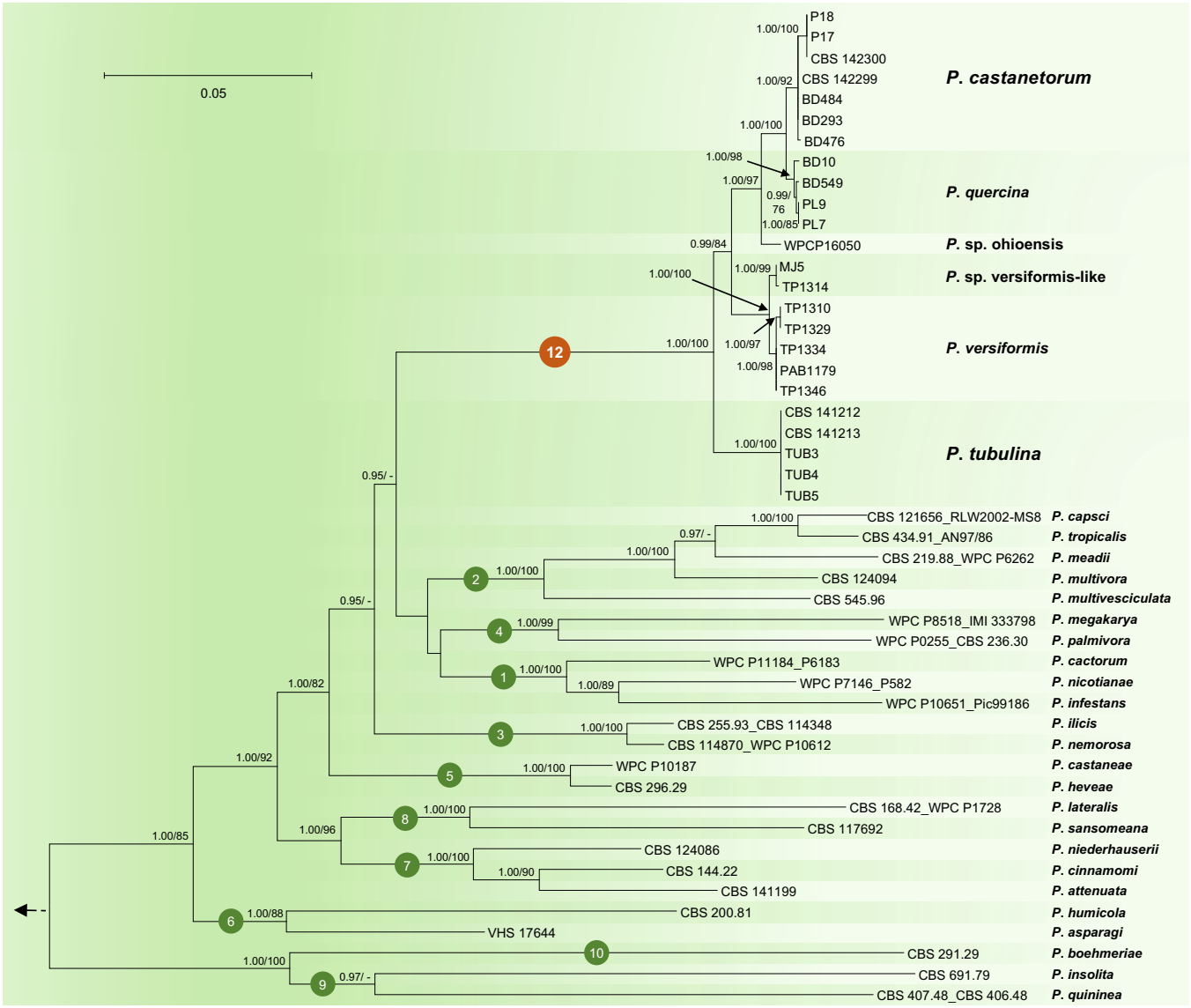

Fig. 1. Fifty percent majority rule consensus phylogram derived from Bayesian inference analysis of four–locus (ITS, Btub, HSP90, NADH1) dataset of the *Phytophthora* Clade 12 and representative species from phylogenetic Clades 1–10. Bayesian posterior probabilities and Maximum Likelihood bootstrap values (in %) are indicated, but not shown below 0.90 and 70 %, respectively. *Nothophytophthora amphigynosa* was used as outgroup taxon (not shown). Bar = 0.05 expected changes per site per branch.

distilled water to remove excess nutrients. In trial 1, 12 plants per *Phytophthora* isolate were planted as pseudo-replicates in 50 x 35 x 27 cm boxes in an autoclaved mixture of peat, vermiculite, and sand (1:1:1 v:v:v). Tubes initially inserted as placeholders in the soil between the individual plants were removed and the holes were filled with the inoculum (*ca* 40 cm3 of inoculum per plant) (Jung *et al*. 2017b). Controls received only rinsed non-infested vermiculite/millet seed/V8-juice mixture at the same rate. In trial 2, ten plants of each *Phytophthora* isolate/ host plant combination were infested in individual pots with the same rate of inoculum as described before. In both trials, plants were incubated for five months in a walk-in growth chamber at 18–20 ºC, 65 % relative humidity, a natural daylight regime, and flooded every 3 wk for 72 h. At the end of the trial, roots were thoroughly washed free from soil. Then, specific symptoms such as root and collar rot lesions and chlorosis and wilting of foliage were recorded.

Two different root damage assessments were used. In trial 1 with *Fagus sylvatica* saplings, the proportion of root damage was assessed visually after spreading the roots uniformly on trays etched with 2 x 2 cm squares according to a scale of five root damage classes: 4 = healthy root system with dense fine root system and well developed tap roots; 3 = < 25 % fine root losses and well developed tap roots; 2 = 26–50 % fine root losses, beginning taproot dieback and small necrotic lesions on woody roots and/or the collar; and 1 = 51–75 % fine root losses, advanced taproot dieback and large necrotic lesions on tap roots and/or the collar; 0 = 76–100 % fine root losses, extensive taproot dieback and girdling necrotic lesions on tap roots and/or the collar. Then roots were dried for 72h at 65 ºC and the dry weights of small woody roots (diam 2–10 mm) and fine roots (diam <2 mm) were recorded for each plant. Data were analysed using one-way ANOVA followed by Dunnett's multiple comparisons test using the programme package Prism 6 (Graphpad, San Diego, CA). In trial 2, *Castanea sativa*, *Quercus ilex,* and *Q. suber* seedlings were removed from the pots and the root system gently washed under tap water (Scanu *et al*.

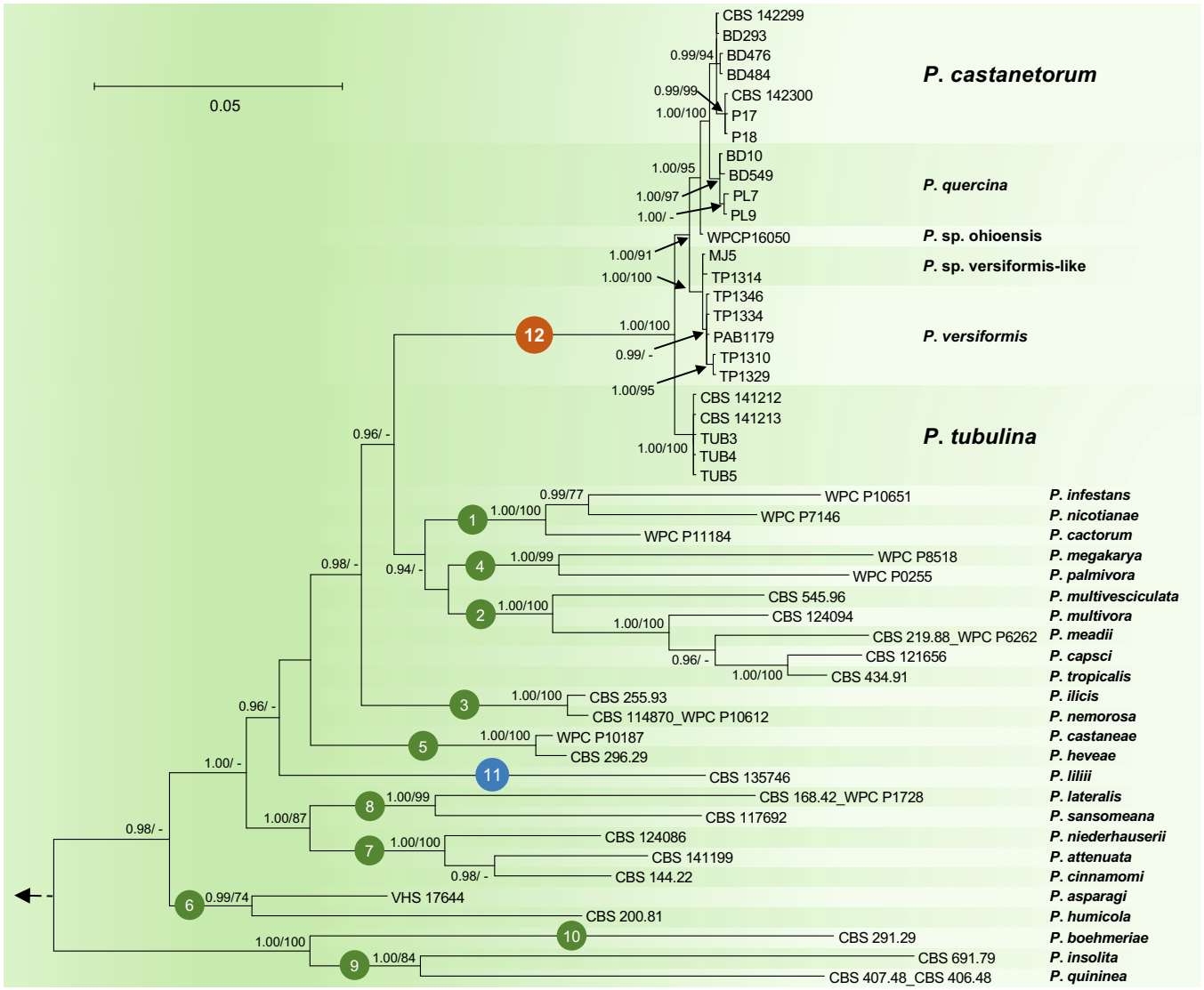

Fig. 2. Fifty percent majority rule consensus phylogram derived from Bayesian inference analysis of nuclear three–locus (ITS, Btub, HSP90) dataset of *Phytophthora* Clade 12 and representative species from phylogenetic Clades 1–11. Bayesian posterior probabilities and Maximum Likelihood bootstrap values (in %) are indicated, but not shown below 0.90 and 70 %, respectively. *Nothophytophthora amphigynosa* was used as outgroup taxon (not shown). Bar = 0.05 expected changes per site per branch.

2014a). Single roots were then cut off at the collar, scanned and total root length for each plant was calculated using the APS Assess 2.0 software (The American Phytopathological Society, St Paul, MN).

In all cases, re-isolations of *Phytophthora* from necrotic tissues were made using selective PARPNH agar (Jung 2009). During each flooding cycle, soils were baited using young leaves of *Ceratonia siliqua*, *F. sylvatica* and *Q. suber* as baits in order to test whether the respective *Phytophthora* species was still active. After each flooding cycle, the water was collected and autoclaved. At the end of the trial boxes were sterilised with bleach and infested substrates and the plants were autoclaved.

RESULTS

Phylogenetic analysis

Sequence datasets of Clade 7a species and species related to *Phytophthora quercina* were analysed separately. All phylogenetic analyses of individual nuclear (ITS, Btub, and HSP90) and mitochondrial (*cox*1 and NADH1) DNA sequences resulted in similar overall tree topologies (data not shown), thus indicating that the individual loci could be combined.

To resolve the phylogenetic positions of *P. castanetorum* and *P. tubulina* within the *P. quercina* clade, and of the latter within the genus *Phytophthora*, a 4-loci dataset (ITS–Btub–HSP90–NADH1) and a nuclear 3-loci dataset (ITS–Btub–HSP90) were analysed separately. Compared to the ML analyses, the BI analyses provided higher support for both terminal clades and the deeper branches. Since the topologies of the BI and ML trees were congruent, the Bayesian trees are presented here (Figs 1–2) with both BI Posterior Probability values and ML bootstrap values shown at the nodes. The resulting phylogenies of the genus *Phytophthora* were rooted to *Nothophytophthora amphigynosa* and were in accordance with several published studies (Blair *et al.* 2008, Martin *et al.* 2014, Rahman *et al.* 2015) with the exception that the inclusion of the two new species *P. castanetorum*

Table 1. Pairwise numbers of different positions along alignments of ITS (842 bp), Btub (911 bp), HSP90 (840 bp), *cox*1 (867 bp) and NADH1 (797 bp) among the taxa from *Phytophthora* Clade 12.

Phytophthora species	*P. castanetorum*					*P. quercina*					*P.* sp. ohioensis					*P.* sp. versiformis					*P.* sp. versiformis-like					*P. tubulina*					Total no. of unique polymorphisms				
	ITS	Btub	HSP90	Cox1	NADH1	ITS	Btub	HSP90	Cox1	NADH1	ITS	Btub	HSP90	Cox1	NADH1	ITS	Btub	HSP90	Cox1	NADH1	ITS	Btub	HSP90	Cox1	NADH1	ITS	Btub	HSP90	Cox1	NADH1	ITS	Btub	HSP90	Cox1	NADH1
P. castanetorum	0	0-3	0	0	0-2	3	0-5	2-3	5-14	4-9	1	2-5	2	n.a.	18-20	2-4	7-10	6	n.a.	30-32	2-3	6-9	6	n.a.	31-33	9	4-7	8	37	39-41	1	0-3	1	5	3-5
P. quercina	3	0-5	2-3	5-14	4-9	0	0-2	0-1	0-9	0-3	2	2-4	2-3	n.a.	15-18	3-5	7-9	6-7	n.a.	30-32	3-4	6-8	6-7	n.a.	32-34	10	4-6	8-9	33-42	37-39	2	0-2	1-2	0-9	1-4
P.* sp. *ohioensis	1	2-5	2	n.a.	18-20	2	2-4	2-3	n.a.	15-18	0	0	0	n.a.	0	1-3	5	4	n.a.	29	1-2	4	4	n.a.	29	8	3	6	n.a.	40	0	0	0	n.a.	4
P.* sp. *versiformis	2-4	7-10	6	n.a.	30-32	3-5	7-9	6-7	n.a.	30-32	1-3	5	4	n.a.	28	0-2	0	0	n.a.	0	0-3	1	0	n.a.	5	9-11	4	4	n.a.	34	0-2	1	0	n.a.	2
***P.* sp. *versiformis*-like**	2-3	6-9	6	n.a.	31-33	3-4	6-8	6-7	n.a.	32-34	1-2	4	4	n.a.	29	0-3	1	0	n.a.	5	0-1	0	0	n.a.	0	9-10	5	4	n.a.	34	0-1	0	0	n.a.	3
P. tubulina	9	4-7	8	37	39-41	10	4-6	8-9	33-42	37-39	8	3	6	n.a.	40	9-11	4	4	n.a.	34	9-10	5	4	n.a.	34	0	0	0	0	0	8	1	3	33	23

n.a. = not available due to insufficient overlap between *cox*1 sequences of *P.* sp. ohioensis, *P. versiformis* and *P.* sp. versiformis-like from GenBank and of *P. castanetorum*, *P. quercina* and *P. tubulina* generated in this study.

Nucleotides missing from the terminal part(s) of partial sequences and undetermined bases (N) were not considered as polymorphisms.

and *P. tubulina* and the three taxa *P.* sp. ohioensis, *P. versiformis,* and *P.* sp. versiformis-like, allowed to resolve the phylogenetic position of the *P. quercina* clade within *Phytophthora*. Together with *P. quercina*, *P.* sp. ohioensis, *P. versiformis,* and *P.* sp. versiformis-like, *P. castanetorum* and *P. tubulina* formed a fully supported monophyletic group (BI posterior probability = 1.00, ML bootstrap = 100 %; Figs 1–2).

Since in the analysis of the nuclear 3-loci dataset *P. lilii* formed a distinct clade (Fig. 2), confirming Rahman *et al.* (2015), the names Clade 11 and Clade 12 are proposed here for *P. lilii* and the new *P. quercina* clade, respectively. In the analyses of both datasets, Clade 12 formed a fully supported group together with Clades 1, 2 and 4, while Clade 3 was basal to this group (Figs 1–2). Within Clade 12, isolates of *P. castanetorum* grouped in a well-supported cluster together with *P. quercina* (posterior probability = 1.00, ML bootstrap = 100 %). *Phytophthora* sp. ohioensis from North America appeared in a basal position of this cluster, while *P. versiformis* and *P.* sp. versiformis-like formed an Australian cluster which grouped in a sister position to the *P. quercina–P. castanetorum–P.* sp. ohioensis cluster (Figs 1–2). *Phytophthora tubulina* appeared in a basal position of Clade 12 (Figs 1–2). In the separate BI and ML analyses of an ITS sequence alignment, *P.* sp. quercina-like, for which only an ITS sequence was available, grouped within Clade 12 (data not shown, but available from TreeBASE: S20982). *Phytophthora castanetorum* differed from the closest taxon *P. quercina* and from *P.* sp. ohioensis in three nuclear (ITS–Btub–HSP90) and the mitochondrial NADH1 gene regions by 9–20 and 23–28 characters, respectively, and from the more distantly related *P. versiformis*, *P.* sp. versiformis-like, and *P. tubulina* by 45–52, 45–51 and 97–102 characters, respectively (Table 1). In addition, in *cox*1 *P. castanetorum* showed differences to *P. quercina* at 5–14 positions (Table 1). Isolates of *P. castanetorum* showed intraspecific variability, with the Sardinian isolates forming a distinct cluster (Figs 1–2). DNA sequences of Sardinian isolates differed from those of *P. castanetorum* from Portugal in Btub and NADH1 by 3 bp and 2 bp, respectively (Table 1). In contrast, *P. tubulina* isolates were identical across all five loci examined. *Phytophthora versiformis* and *P.* sp. versiformis-like showed differences to each other at 6–9 positions, and to *P. castanetorum* and *P. quercina* at 45–52 and 46–53 positions, respectively (Table 1). The basal species *P. tubulina* differed from *P. castanetorum*, *P. quercina*, *P.* sp. ohioensis, *P. versiformis* and *P.* sp. versiformis-like by 97–102, 92–106, 57, 51–53 and 52–53 characters, respectively (Table 1). In addition, *P. tubulina* was separated from *P. castanetorum* and *P. quercina* in *cox*1 by 37 and 33–42 characters, respectively (Table 1).

Bayesian and ML analyses of the combined five locus dataset for Clade 7a generated trees with essentially the same topology. The Bayesian analysis provided more support for deeper branches, while support for terminal clades and their clustering was equivalent in both analyses. The Bayesian tree is shown in Fig. 3 with both BI posterior probability and ML bootstrap values provided at the nodes (Fig. 3). The resolution was good at terminal clades and allowed for the differentiation of 17 distinct lineages within Clade 7a corresponding to 14 described species, *P. attenuata*, *P. europaea*, *P. flexuosa*, *P. formosa*, *P. intricata*, *P. fragariae*, *P. rubi*, *P. uliginosa*, *P.*

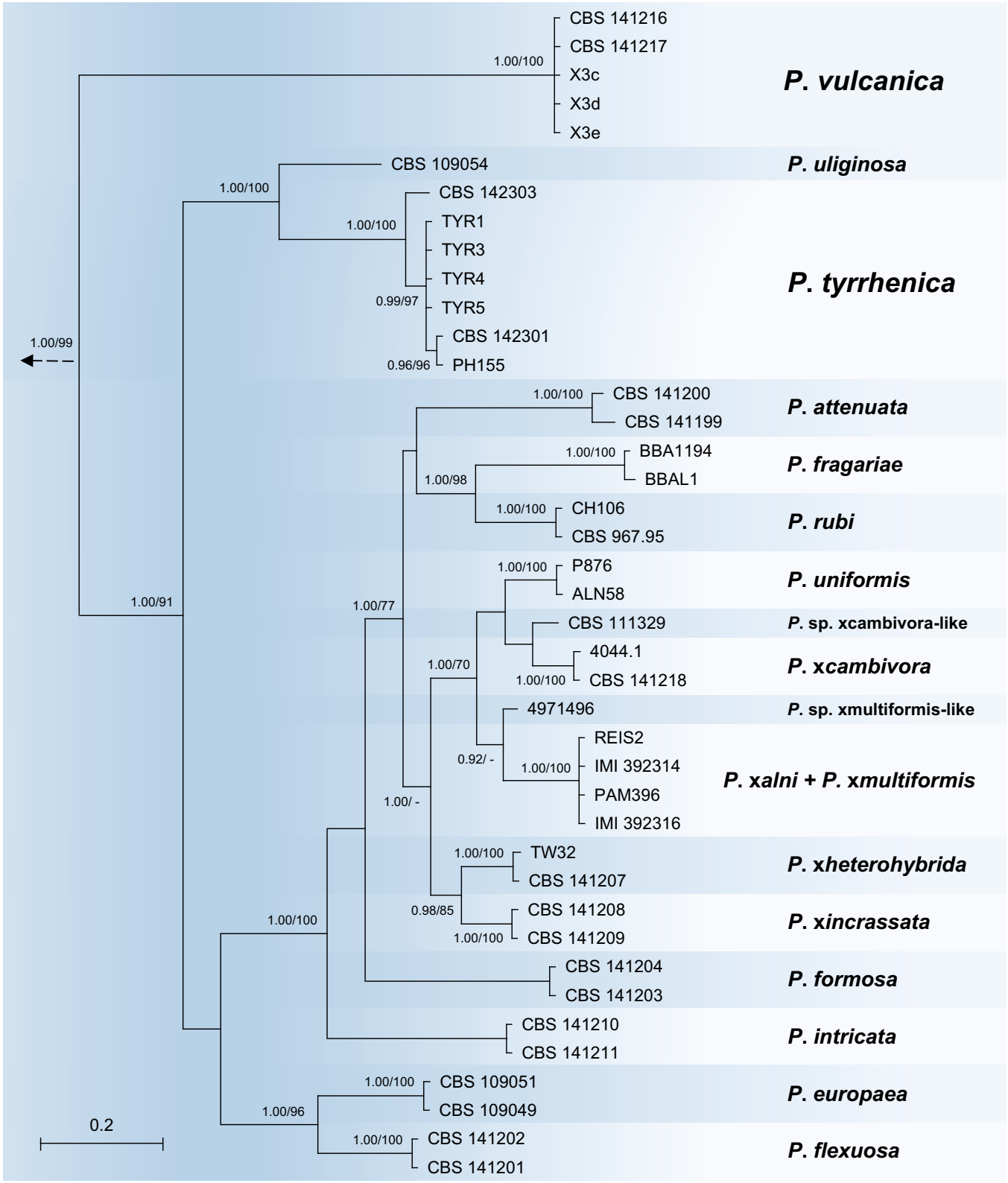

Fig. 3. Fifty percent majority rule consensus phylogram derived from Bayesian phylogenetic analysis of five–locus (ITS, Btub, HSP90, *cox*1, NADH1) dataset of Clade7a. Bayesian posterior probabilities and Maximum Likelihood bootstrap values (in %) are indicated, but not shown below 0.90 and 70 %, respectively. *Phytophthora cinnamomi* and *P. niederhauserii* from Clade 7b were used as outgroup taxa (not shown). Bar = 0.05 expected changes per site per branch.

uniformis, *P.* x*cambivora*, *P.* x*heterohybrida*, *P.* x*incrassata*, *P.* x*alni* / *P.* x*multiformis*, the two informally designated taxa *P.* sp. x*cambivora*-like and *P.* sp. x*multiformis*-like, and the two new species *P. tyrrhenica* and *P. vulcanica* described in this study (Fig. 3). Isolates of *P. tyrrhenica* grouped together with *P. uliginosa* in a well-supported clade (posterior probability = 1.00, ML bootstrap = 100 %), both species being separated by 2, 4 and 1–2 characters in ITS, Btub and HSP90, respectively, and by 22–24 and 8–10 characters in *cox*1 and NADH1, respectively. The relative phylogenetic position

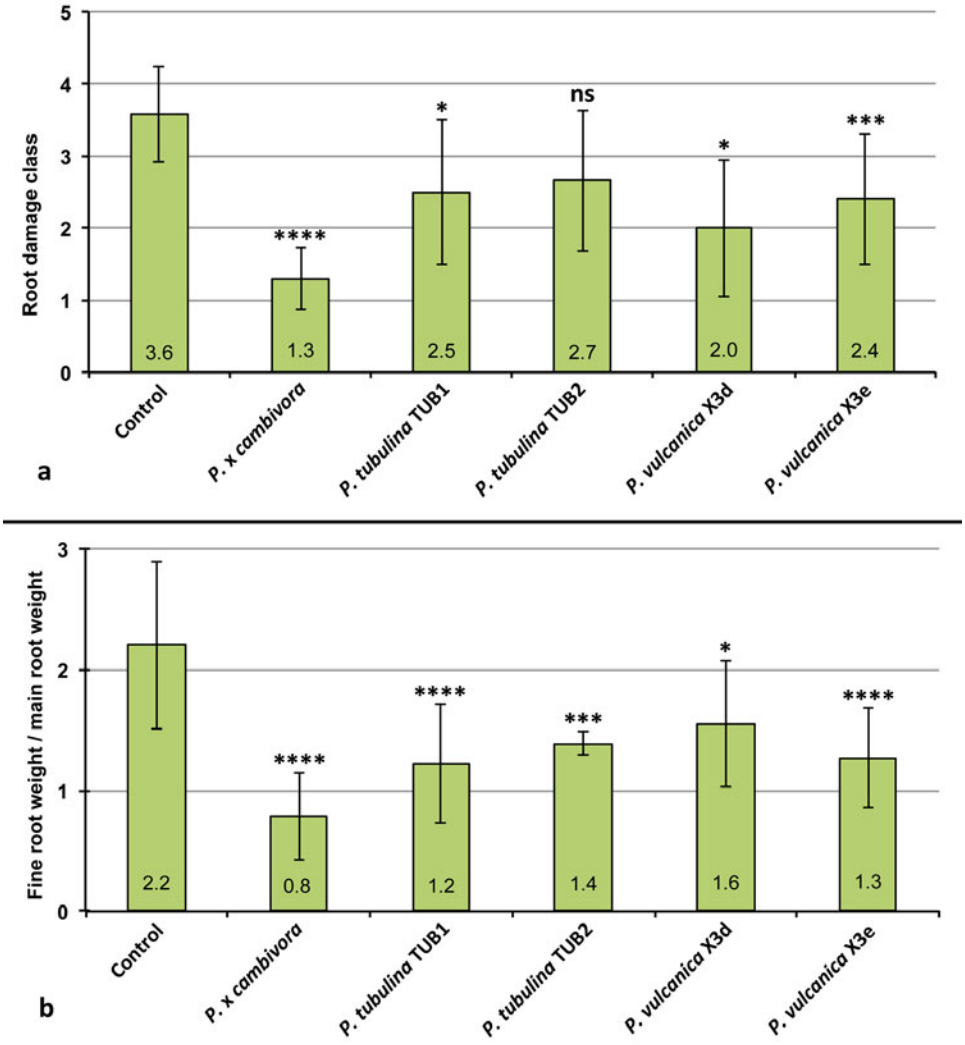

Fig. 4. Mean root damage class and mean fine root weight / main root weight ratio of 3–year–old *Fagus sylvatica* plants after 5 months growth in uninfested soil (control) and in soil infested by *Phytophthora* x*cambivora* (CBS 141218), *P. tubulina* (CBS 141212, CBS 141213) and *P. vulcanica* (X3d, X3e), respectively. Bars show standard deviations; asterisks represent statistical significances (* = P < 0.05, ** = P < 0.01, *** = P < 0.001, **** = P < 0.0001), ns = not significant.

of *P. tyrrhenica* and *P. uliginosa* was also well-supported (Fig. 3). The *P. tyrrhenica–P. uliginosa* clade grouped in a sister position to the remaining in-group taxa representing 15 taxa from Clade 7a (Fig. 3). Small intraspecific variation of up to seven characters across the five gene regions was found amongst *P. tyrrhenica* isolates, which was related to different oak species and geographic origin. Isolate PH103 (from *Quercus suber* in Sardinia) represented a distinct basal lineage (Fig. 3). In contrast, *P. vulcanica* was monomorphic across all five loci examined, suggesting that the tested isolates could belong to the same clone of the species. Across the five DNA regions, *P. vulcanica* showed differences to its closest relatives *P. uliginosa* and *P. tyrrhenica* at 109 and 109–114 positions, respectively, and resided in a well-supported basal position of the whole Clade 7a (Fig. 3).

Hosts and geographic distribution

Phytophthora castanetorum was exclusively isolated from *Castanea sativa* forests in Portugal, at Monchique (N 37° 18.851', W 8° 32.455'; 496 m above sea level, asl) and in the Parque Natural Serra da Estrela (N 40° 25.489, W 7° 22.523'; 901 m asl), and in Sardinia at Gennargentu montain (N 39° 56.946', E 9° 11.387'; 858 m asl). It usually co-occurred with *P.* x*cambivora* and *P. cinnamomi*, associated with severe ink disease symptoms. *Phytophthora tubulina* was isolated alongside *P.* x*cambivora* and *P. plurivora* from mildly declining *Fagus sylvatica* trees in the Dunkelsteiner Forest in Austria (N 48° 14.561', E 15° 28.276'; 497 m asl), while *P. vulcanica* was recovered from relatively healthy *F. sylvatica* trees at Timpa Rossa on Mount Etna in Sicily (N 37° 48.849', E 15° 1.407'; 1862 m asl). *Phytophthora tyrrhenica* was associated with declining *Quercus ilex* and *Q. suber* trees in different forest stands on the Italian islands Sardinia (N 40° 52.492', E 9° 2.720'; 183 m asl) and Sicily (N 37° 54.341', E 14° 4.490'; 1110 m asl).

Soil infestation trials

Pathogenicity on Fagus sylvatica *seedlings (trial 1)*

At the end of the trial shoots and root systems of control plants of *F. sylvatica* were generally healthy and well developed with a fine root/main root weight (frw/mrw) ratio of 2.2 and a root damage class of 3.6 ± 0.67 (Fig. 4). *Phytophthora* x*cambivora* was the most aggressive species causing after 5 months 50 % mortality, a frw/mrw ratio of 0.78 ± 0.36 (64.5 % reduction compared to the control), 54.4 % reduction of fine

root weight compared to control plants and a root damage class of 1.3 ± 0.14 (i.e. 67.5 % fine root losses and advanced dieback and necrotic lesions of tap roots and root collars) (Fig. 4). *Phytophthora tubulina* isolates (TUB1= CBS 141212 and TUB2= CBS 141213) caused 8.3 and 16.6 % mortality, a frw/mrw ratio of 1.22 ± 0.49 and 1.39 ± 0.1 (44.5 and 36.8 % reduction compared to the control), and a root damage class of 2.5 ± 1.0 and 2.7 ± 1.0, respectively (Fig. 4). Beech plants in soil infested by isolates X3d and X3e of *P. vulcanica* had a frw/mrw ratio of 1.55 ± 0.52 and 1.27 ± 0.41 (29.8 and 42.3 % reduction compared to the control), and a root damage class of 2.0 ± 0.95 and 2.4 ± 0.9, respectively (Fig. 4). Both isolates caused 8.3 % mortality and, chlorosis and wilting in 58.3 % (X3d) and 75 % (X3e) of the plants. Differences of root damage class and frw/mrw ratio to the control were statistically significant for *P.* x*cambivora*, both isolates of *P. vulcanica* and isolate TUB1 of *P. tubulina* (Fig. 4). For *P. tubulina* isolate TUB 2, the difference to the control was only significant for the frw/mrw ratio but not for the root damage class (Fig. 4).

Pathogenicity on Castanea sativa *seedlings (trial 2)*

At the end of the experiment seedlings inoculated with *P.* x*cambivora* were mostly dead (mortality rate above 80 %) or showed severe wilting associated with collar and root necrosis. In contrast, all seedlings inoculated with *P. castanetorum* were alive and showed only weak symptoms of wilting and chlorosis of leaves. Control plants did not show any aboveground symptoms and exhibited overall faster growth. *Phytophthora* x*cambivora* was extremely aggressive to the root systems causing more than 60 % reduction of total root length ($P < 0.0001$). In contrast, seedlings inoculated with *P. castanetorum* showed only mild fine root infections but no symptoms of woody root and collar infections, and total root length did not differ statistically from the control plants (Fig. 5).

Pathogenicity on Quercus ilex *and* Quercus suber *seedlings (trial 2)*

Oak seedlings inoculated with *P. tyrrhenica* started to show symptoms of leaf chlorosis and shoot dieback 45 d post-inoculation. Mortality of seedlings occurred between the third and fourth month after inoculation. Based on mortality rates after five months, *P. cinnamomi* was more aggressive than *P. tyrrhenica* on both *Q. ilex* and *Q. suber*, killing 80 % and 63.5 % of seedlings, respectively, whereas *P. tyrrhenica* caused an average mortality on *Q. ilex* and *Q. suber* of 48.5 % and 25 %, respectively. On *Q. ilex*, both *Phytophthora* species caused fine root losses and necrosis of mother roots, and a significant reduction in root length compared to control seedlings ($P < 0.0001$) (Fig. 5). *Phytophthora cinnamomi* caused significantly higher root reduction than *P. tyrrhenica* for which Dunnett's test revealed no significant differences in total root length of inoculated seedlings. Also on *Q. suber*, both *P. cinnamomi* and *P. tyrrhenica* caused significant total root length reduction, but the reduction by *P. cinnamomi* was significantly higher from that caused by both isolates of *P. tyrrhenica* ($P < 0.0001$) (Fig. 5).

At the end of all pathogenicity trials, each *Phytophthora* species could be re-isolated from both infested soils using young leaves of *C. siliqua*, *F. sylvatica* and *Q. suber* as baits and necrotic fine roots or necrotic root lesions by direct plating onto PARPNH agar. No *Phytophthora* species could be isolated from soil and roots of control plants.

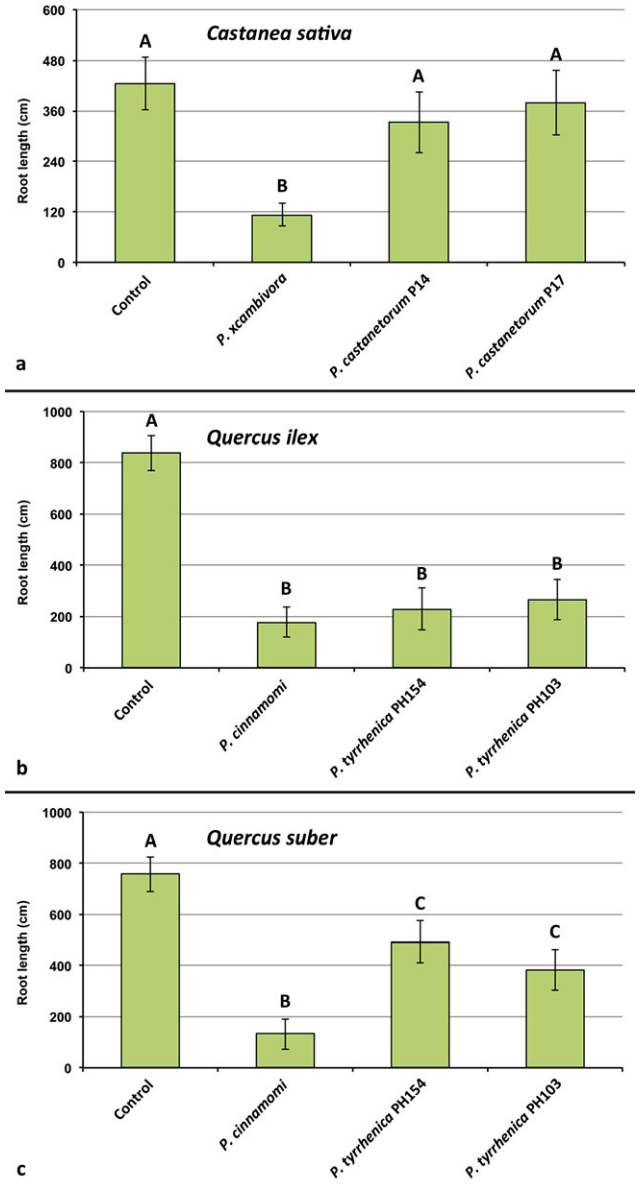

Fig. 5. Mean root length of 1–year–old plants of *Castanea sativa*, *Quercus ilex* and *Q. suber* after 5 months growth in uninfested soil (control) and in soil infested by *Phytophthora* x*cambivora* (CBS 141218), *P. castanetorum* (CBS 142300, P17), *P. cinnamomi* (PH069) and *P. tyrrhenica* (CBS 142301, CBS 142303), respectively. Bars show standard deviations; asterisks represent statistical significances (* = P < 0.05, ** = P < 0.01, *** = P < 0.001, **** = P < 0.0001), ns = not significant.

TAXONOMY

Morphological and physiological characters and measurements of the four new *Phytophthora* taxa and related species are given in the comprehensive Table 2.

Table 2. Morphological characters and dimensions (µm), cardinal temperatures (°C) and temperature-growth relations (mm/d) on V8A of *Phytophthora castanetorum*, *P. tyrrhenica*, *P. tubulina*, *P. vulcanica* and their closest relatives in phylogenetic Clades 7a and 12, respectively. Most discriminating characters are highlighted in bold.

	P. castanetorum	***P. tubulina***	***P. quercina***	***P. tyrrhenica***	***P. vulcanica***	***P. uliginosa***	***P. europaea***	***P. flexuosa***
No. of isolates	9	5	10 [b]	7	5	3[a]	7[a]	3[a]
Sporangia	ovoid, subglobose, obpyriform, globose, (ellipsoid, distorted)	ovoid, obpyriform, distorted, (globose, subglobose, ellipsoid, limoniform)	subglobose, ovoid, obpyriform, peanut, ampulliform, distorted	**elongated ellipsoid**, elongated ovoid, elongated limoniform	ovoid, ellipsoid, (obpyriform, pyriform)	**ellipsoid**, ovoid, peanut-shaped, (obpyriform, limoniform)	ovoid, obpyriform, ellipsoid, (subglobose),	ovoid, ellipsoid, (obpyriform, limoniform)
apex	77.4 % papillate, 14.9 % semipapillate; **7.7 % nonpapillate**, 4.9 % curved	78 % mono-, bi- or tripapillate; 13.3 % semi-papillate; **8.7 % non-papillate**, 4.9 % curved	**all papillate**, some bi- and tripapillate; often curved	nonpapillate	nonpapillate	nonpapillate	nonpapillate, **often pointed**	
lxb mean	47.0±5.7 x 36.6±3.7	**51.6±9.8 x 37.3±7.0**	42.4±11.5 x 29.3±13.8	**68.4±1.7 x 28.9±1.9**	57.3±8.7 x 34.5±4.2	**67.0±8.5 x 42.4±6.4**	63.7±16.9 x 44.6±8.3	56.1±7.4 x 36.7±5.2
range of isolate means	44.2–48.1 x 35.4–38.3	43.3–57.8 x 31.2–45.0	36.0–49.2 x 23.3–33.7	**66.1–70.0 x 27.5–31.9**	53.6–61.0 x 31.8–36.4	**65.7–70.3 x 30.9–44.4**	50.0–78.9 x 36.7–51.2	53.3–58.6 x 33.9–39.4
total range	27.1–74.5 x 18.1–47.9	29.5–98.5 x 19.2–59.2	18.8–112.5 x 13.8–47.5	45.3–110.2 x 16.2–39.4	35.5–80.7 x 22.5–42.9	41.1–85.0 x 24.8–56.9	23.6–124.3 x 21.9–67.3	34.9–74.8 x 22.8–49.7
l/b ratio	**1.29** ± 0.15	1.40 ± 0.18	1.45 ± 0.37	2.40 ± 0.18	1.67 ± 0.22	1.60 ± 0.19	1.42 ± 0.19	1.54 ± 0.18
caducity	–	**rare**	–	–	–	–	–	–
lateral insertion	37.7 %	22.4 %	frequent					
exit pores	7.0 ± 1.1	6.4 ± 1.2	6.5 ± 1.2	12.1 ± 2.4	17.0 ± 3.0	15.4 ± 3.4	19.3 ± 4.7	19.7 ± 3.4
zoospore cysts	9.2 ± 1.0	11.7 ± 1.8	9.5 (7.1–12.9)	14.6 ± 2.3	10.0 ± 1.2	11.9 ± 1.8	15.3 ± 2.0	13.3 ± 1.3
Breeding system	homothallic	homothallic	homothallic	homothallic	homothallic	homothallic	homothallic	homothallic
Oogonia								
mean diam	**32.9** ± 3.0	29.2 ± 4.4	29.4 ± 4.1	**37.2** ± 3.3	**35.8** ± 3.6	**46.2** ± 7.5	37.3 ± 5.4	36.8 ± 3.3
range of isolate means	30.5–34.4	25.4-30.1	25.8–32.0	36.8–40.9	33.6–36.5	41.6–53.3	34.4–39.9	36.0-38.3
total range	24.3–41.7	16.5–42.5	19.0–45.0	25.0–39.3	23.0–46.0	17.9–65.5	19.2–48.4	25.7–42.8
tapering base	**61.3 %** (40–86 %)	48.7 % (30–78 %)	n.a.	**–**	**37.3 %** (8–60 %)	**–**	**60.0 %** (52–81 %)	47.9 % (32–58 %)
elongated	**65.4 %** (50–82 %)	59.5 % (36–86 %)	**45 %** (10–86 %)	**–**	**44.8 %** (8–80 %)	**–**	21.3 % (12–34 %)	19.7 % (4–36 %)
tubular	**–**	**24.5 %** (21–28 %)	**–**	–	**–**	–	–	–
excentric	6.7 % (2–20 %)	5.0 % (2–8 %)	n.a.	–	**20.9 % (**9–46 %)	–	4.0 % (0–8 %)	5.3 % (2–10 %)
smooth-walled	100 %	100 %	100 %	100 %	100 %	100 %	100 %	**34.4 %** (19–48 %)
Oospores								
plerotic oospores	**64.3 %** (50–83 %)	**44 %** (24–76 %)	mostly aplerotic	**>99 %** (99–100 %)	27.3 % (10–45 %)	**30.0 %** (12-46 %)	**46.3 %** (38–53 %)	**>99 %** (99–100 %)

Table 2. (Continued).

	P. castanetorum	*P. tubulina*	*P. quercina*	*P. tyrrhenica*	*P. vulcanica*	*P. uliginosa*	*P. europaea*	*P. flexuosa*
mean diam	28.7 ± 2.6	26.1 ± 3.7	24.7 ± 2.6	**33.7**±1.3	30.5 ± 3.2	**41.3**±6.1	33.2 ± 5.3	32.2 ± 2.7
Total range	21.9–38.8	15.7–36.3	18.0–30.0	24.6–39.9	19.7-38.2	12.5-55.0	16.3–45.1	22.7–37.7
wall diam	3.1 ± 0.49	2.0 ± 0.6	2.4 ± 0.56	**2.9** ± 1.5	2.4 ± 0.4	**4.2** ± 0.7	2.5 ± 0.7	3.1 ± 0.5
oospore wall index	0.51 ± 0.05	0.38 ± 0.08	0.44 ± 0.1	0.41 ± 0.03	0.40 ± 0.06	**0.49** ± 0.07	0.38 ± 0.06	**0.47** ± 0.06
Abortion rate	**21.5 %** (18–29 %)	**72.3 %** (40–91 %)	**<10 %**	5 % (3–7 %)	**52.8 %** (0–80 %)	6.2 % (3-10 %)	**24.9 %** (18–31 %)	**1.7 %** (1–2 %)
Antheridia	**99 % paragynous**	**100 % paragynous**	**100 % paragynous**	100 % paragynous	**4.7 % amphigynous**	100 % paragynous	100 % paragynous	100 % paragynous
size	14.0±2.3 x 10.2±1.6	14.9±3.1 x 10.9±1.7	16.6±6.3 x 12.7±2.5	16.9±4.6 x 12.8±0.13	16.3±3.1 x 12.6±2.3	16.9±3.1 x 13.3±2.5	13.6±2.6 x 10.8±2.1	13.4±2.1 x 10.0±1.7
Chlamydospores	**globose**	**–**	**rare, in some isolates**	–	–	–	–	–
mean diam	29.5 ± 4.9 (17.7–47.0)		17–35					
Hyphae	Sympodial branching with protruding tip of mother hypha	Sympodial branching with protruding tip of mother hypha	Sympodial branching with protruding tip of mother hypha		**Often inflated tubular or club-shabed**			**Coralloid**
Hyphal aggregations	–	–	–	–	**+**	(+)	–	**–**
Hyphal swellings	in water; globose, subglobose, limoniform; some catenulate	in water; subglobose, triangular; some catenulate	**–**	**in water; subglobose, irregular, catenulate**	in water; subglobose, irregular, catenulate	**in water; subglobose, irregular, catenulate**	**–**	–
Maximum temperature	25–<30	25–<30	27.5	**25–<30**	**25–<30**	**25**	30–<35	35
Optimum temperature	**20**	**20**	25	**25**	**15**	20	25	25
Growth rate at optimum	2.9 ± 0.91	**1.7 ± 1.0**	3.7	1.1 ± 0.4	1.0 ± 0.1	1.2 ± 0.2	4.9 ± 0.53	4.7 ± 0.61
Growth rate at 20°C	2.7 ± 0.75	**1.7 ± 1.0**	3.3	1.5 ± 0.3	0.9 ± 0.04	1.2 ± 0.2	4.4 ± 0.59	4.4 ± 0.56

– = character not observed; + = character observed; n.a. = not available.

[a] Data from Jung *et al*. (2017b).

[b] Morphological and morphometric data from Jung *et al*. (1999); standard deviations of all morphometric data, oospore wall diameter and oospore wall index calculated from original dataset.

Phytophthora castanetorum T. Jung, M. Horta Jung, Bakonyi & Scanu, **sp. nov.**
MycoBank MB819699
(Fig. 6)

Etymology: Referring to the association of this species with forests of *Castanea sativa* (*Castanetum* is the phytosociological term for a chestnut forest).

Diagnosis: *Phytophthora castanetorum* differs from all other *Phytophthora* species from Clade 12 by regularly producing chlamydospores, and from *P. quercina* also by producing a low proportion of semipapillate and nonpapillate sporangia.

Type: **Portugal:** *Algarve*: Monchique, isolated from rhizosphere soil of a mature *Castanea sativa* tree, March 2015, *T. Jung* (CBS H-22983–holotype, dried culture on V8A; CBS 142299 = BD 292–ex-type culture). ITS and *cox*1 sequences GenBank MF036182 and MF036266, respectively.

Description: *Sporangia, hyphal swellings and chlamydospores* (Fig. 6A–G): *Sporangia* commonly observed in solid agar of older cultures (Fig. 6A) and produced abundantly in non-sterile soil extract; typically borne terminally on unbranched sporangiophores or in irregular lax or regular dense sympodia, and some formed on short lateral hyphae (Fig. 6H) or intercalary (Fig. 6I); non-caducous, monopapillate (77.4 %; Fig. 6A–G), very rarely bipapillate (over all isolates <1 %), semipapillate (14.9 %; Fig. 6H) or non papillate (7.7 %; Fig. 6I), and often forming a conspicuous basal plug that protrudes into the empty sporangium (Fig. 6J); in solid agar with conspicuously protruding papillae (Fig. 6A); sporangial shapes very variable, ovoid (over all isolates 77.4 %; Fig. 6B–D, I–J) or subglobose to globose (11.7 %; Fig. 6G) to obpyriform (4.6 %; Fig. 6E), ellipsoid (2.0 %), limoniform (1.0 %; Fig. 6A, F), or distorted (3.3 %); unusual features such as lateral attachment of the sporangiophore (over all isolates 37.7 %; Fig. 6D, G), hyphal extensions (9.1 %; Fig. 6B, D), markedly curved apices (4.9 %) or the presence of a vacuole (8.0 %; Fig. 6B–G) common in all isolates. Small subglobose to limoniform hyphal swellings sometimes formed close to the sporangial base (Fig. 6C). *Zoospores* discharged through an exit pore 4.0–9.5 µm wide (av. 7.0 ± 1.1 µm) (Fig. 6J), limoniform to reniform whilst motile, becoming spherical (av. diam = 9.2 ± 1.0 µm) on encystment, direct germination common in older water cultures (Fig. 6L). Sporangia of seven isolates averaged 47.0 ± 5.7 × 36.6 ± 3.7 µm (overall range 27.0–74.5 × 18.0–48.0 µm) with a range of isolate means of 44.2–48.1 × 35.4–38.3 µm and a length/breadth ratio of 1.29 ± 0.15 (range of isolate means 1.25–1.36). *Swellings* commonly observed in liquid culture; 27.1 ± 9.9 µm diameter (total range 10.0–47.0 µm), subglobose to globose, liminiform, pyriform or distorted; sometimes catenulate and often with individual or radiating hyphal extensions, (Fig. 6P–Q). *Chlamydospores* globose, produced on both CA and V8A, 29.5 ± 4.9 µm diam (total range 18.0–47.0 µm) (Fig. 6R).

Oogonia, oospores, antheridia and hyphae (Fig. 6H–O): *Gametangia* readily produced in single culture by all isolates on V8A within 7-10 d. *Oogonia* terminal, smooth-walled, and elongated pyriform to ellipsoid (on av. 65.4 %; Fig. 6N–O) or globose to slightly subglobose (34.6 %; Fig. 6K–M); bases often tapering (61.3 %; Fig. 6K, N–O) and sometimes slightly curved (4.9 %; Fig. 6O); mean 32.9 ± 3.0 µm diam (overall range 24.5–41.5 µm and range of isolate means 30.5–34.5 µm) and an average length of 40.5 ± 4.6 µm; almost plerotic (53.1 %) or aplerotic (46.9 %). *Oospores* usually globose (98.3 %; Fig. 6K–N) but could be slightly elongated in elongated oogonia (1.7 %; Fig. 6O); thick-walled, wall thickness 3.1 ± 0.5 µm (range 1.8–4.5 µm), and oospore wall index 0.51 ± 0.05.; abortion 19-24 % after 4 wk increasing to 58-91 % after 12 months. *Antheridia* almost exclusively paragynous and club-shaped to subglobose (Fig. 6K–L, N), sometimes with one or more finger-like projections (4.3 %), but a few amphigynous antheridia observed in all isolates (Fig. 6M). *Primary hyphae* often branched in a mono- or dichasium with the mother hypha ending in a short protruding tip (Fig. 6S–T).

Cultures (Figs 11, 13): *Colonies* on CA stellate with limited aerial mycelium and on V8A uniform and woolly; on PDA and MEA isolates formed uniform colonies, dense felty on PDA and mostly submerged on MEA. All isolates with very slow growth on PDA and MEA (Fig. 11). Temperature-growth relations are shown in Fig. 13. All six isolates included in the growth test had similar growth rates. The maximum growth temperature was 25–30 °C, with no grow when plates incubated for 5 d at 30 °C were transferred to 20 °C. Average radial growth rate at the optimum temperature of 25 °C 3.7 mm/d.

Additional material examined: **Portugal:** *Beira Alta*: Parque Natural da Serra da Estrela, isolated from rhizosphere soil of a mature

Fig. 6. *Phytophthora castanetorum*. **A**. papillate limoniform sporangium formed in solid V8 agar (V8A) (CBS 142299 — ex-type). **B–J.** Sporangia formed on V8A flooded with soil extract. **B–G.** With vacuole. **B.** Ovoid, papillate with external proliferation close to sporangial base and hyphal extension (arrow) (BD 484). **C.** Ovoid, papillate with limoniform swelling before sporangial base (CBS 142299). **D.** Ovoid, papillate with laterally attached sporangiophore (BD 484). **E.** Obpyriform, papillate with short hyphal extension (arrow) (CBS 142299). **F.** Limoniform, papillate with elongated base and conspicuous basal plug (BD 486). **G.** Globose, papillate with laterally attached sporangiophore (BD 484). **H.** Ovoid, semipapillate on short lateral hypha (BD 476). **I.** ovoid, nonpapillate intercalary (BD 336). **J.** Ovoid sporangium with conspicuous basal plug, releasing zoospores (CBS 142299). **K–O.** Mature oogonia containing thick-walled oospores with large ooplast, formed in single culture in V8A. **K–L.** Globose to subglobose with aplerotic oospore and paragynous antheridium (CBS 142299). **M.** Globose to subglobose with aplerotic oospore and amphigynous antheridium (BD 484). **N.** Elongated excentric with aplerotic oospore and paragynous antheridium (BD 484). **O.** Elongated pyriform with paragynous antheridium, curved base and plerotic elongated oospore with two ooplasts (CBS 142299). **P–R.** Hyphal swellings formed on V8A flooded with soil extract (CBS 142299). **P.** Peanut-shaped intercalary. **Q.** Pyriform, terminal with radiating hyphal extensions. **R.** Globose, terminal with short hyphal extension. **S–T.** Sympodially branching primary hyphae in solid V8A with the mother hypha ending in a short protruding tip (CBS 142299). Bar A-T = 25 µm.

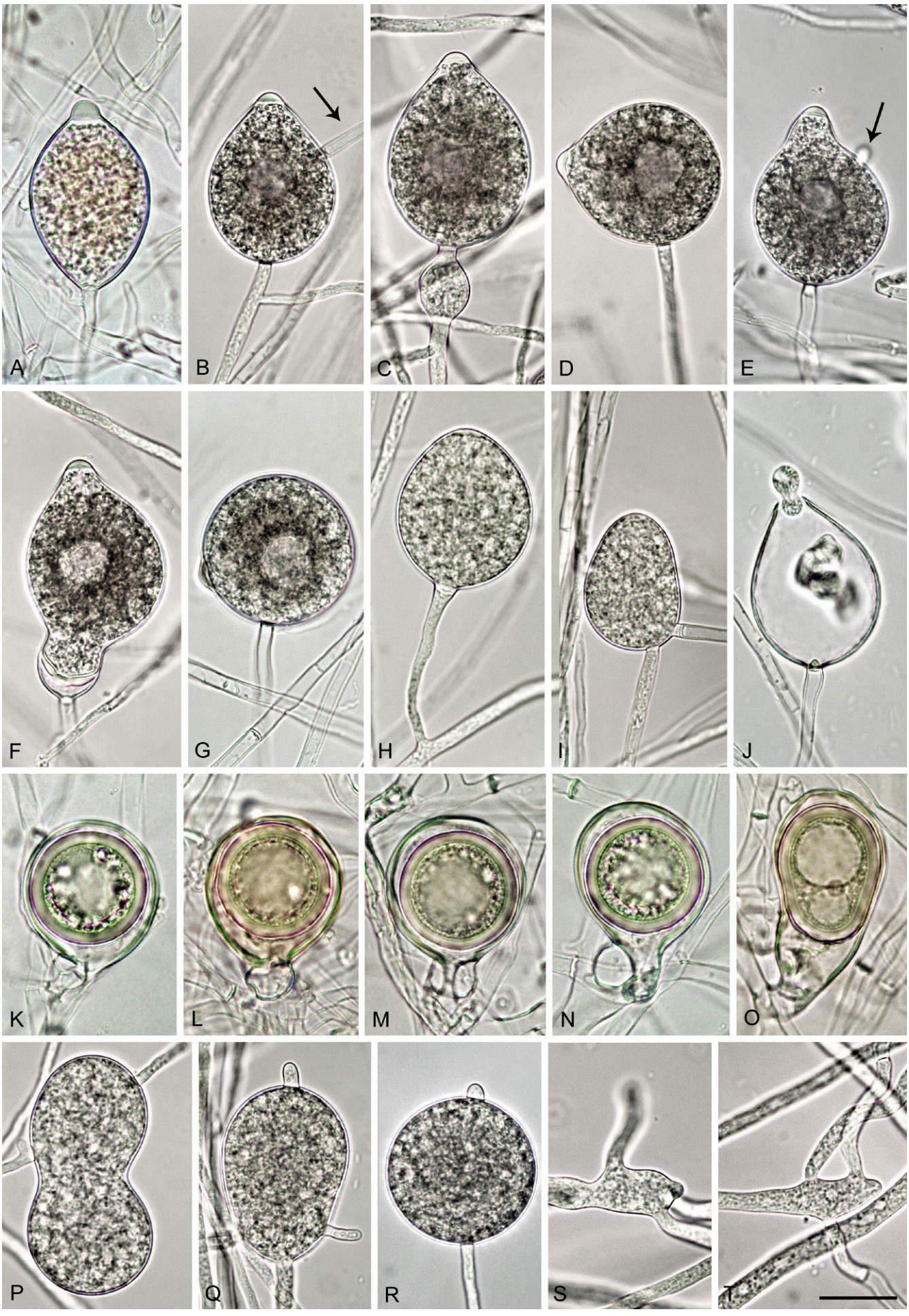
A
B
C
D
E
F
G
H
I
J
K
L
M
N
O
P
Q
R
S
T

Castanea sativa tree, June 2015, *T. Jung* (BD 476,484, 485, 486); *Algarve*: Serra de Monchique, isolated from rhizosphere soil of a mature *C. sativa* tree, March 2015, *T. Jung* (BD 293).–**Italy**: *Sardinia*; Gennargentu mountain, isolated from rhizosphere soil of a coppiced *C. sativa* tree, May 2014, *B. Scanu & S. Seddaiu* (CBS 142300 = P14, P17, P18).

Phytophthora tubulina T. Jung, T. Cech, Scanu, Horta Jung & Bakonyi, **sp. nov.**
MycoBank MB819701
(Figs 7–8)

Etymology: Name refers to the tubular shape of many oogonia (tubulina Lat., tubular).

Diagnosis: *Phytophthora tubulina* differs from all other known *Phytophthora* species by having partially extremely elongated, often tubular oogonia with high oospore abortion rates, and from *P. quercina* by producing a low proportion of semipapillate and nonpapillate sporangia.

Type: **Austria:** *Lower Austria*; Dunkelsteiner Forst, isolated from rhizosphere soil of a mature *Fagus sylvatica* tree, Sept. 2010, *T. Jung* (CBS H-22557–holotype, dried culture on V8A; CBS 141212 = TUB1–ex-type culture). ITS and *cox*1 sequences GenBank MF036196 and MF036277, respectively.

Description: *Sporangia*, *hyphal swellings and chlamydospores* (Fig. 7A–U): *Sporangia* infrequently observed in solid agar, abundantly produced in non-sterile soil extract; borne terminally on unbranched sporangiophores, in lax sympodia, on short lateral sporangiophores (Fig. 7B, O) or intercalary (3.4 %; Fig. 7L); sometimes formed on short hyphal appendices growing from mature sporangia (Fig. 7N); usually non-caducous (Fig. 7A–L, N, R–S) but a low proportion (<1 %) of caducous sporangia without preformed pedicels (Fig. 7O-Q) present in most isolates; apices highly variable ranging from monopapillate (56.6 %; Fig. 7A–G, N, P), bi- or tripapillate (21.4 %; Fig. 7H–I, Q), semipapillate (13.3 %; Fig. 7J) to nonpapillate (8.9 %; Fig. 7K–L, O); sometimes curved (4.9 %; Fig. 7C, G); sporangial shapes ranging from ovoid or elongated ovoid (69.4 %; Fig. 7A–B, E), obpyriform (15.3 %; Fig. 7C), limoniform (3.0 %; Fig. 7D), subglobose (3.7 %) or less frequently ellipsoid and globose (2.3 %) to distorted shapes (6.3 %; Fig. 7H–I, Q); hyphal appendices (6.7 %; Fig. 7K, O) and laterally attached sporangiophores (22.4 %; Fig. 7B, E, N–O) commonly observed; dimensions of six isolates of *P. tubulina* averaging 51.6 ± 9.8 x 37.3 ± 7.0 µm (overall range 29.5–98.5 x 19.0–59.0 µm) with a range of isolate means of 43.5–58.0 x 31.0–45.0 µm; length/breadth ratio 1.4 ± 0.18 with a range of isolate means of 1.27–1.49; sporangial germination directly (Fig. 7R) or more often indirectly with zoospores discharged through an exit pore 4.0–9.0 µm wide (av. 6.4 ± 1.2 µm) (Fig. 7S). *Zoospores* limoniform to reniform whilst motile, becoming spherical (av. diam = 11.7 ± 1.8 µm) on encystment. *Swellings* subglobose to liminoform, often catenulate and with radiating hyphae, infrequently produced on sporangiophores (Fig. 7M, T–U). *Chlamydospores* not observed.

Oogonia, oospores, antheridia and hyphae (Fig. 8A–S): *Gametangia* readily produced in single culture by all isolates of *P. tubulina* on V8A within 10 d. *Oogonia* borne terminally or laterally, with smooth walls and tapering, often long bases (on av. 53.2 %; Fig. 8A–E, G, K); globose to subglobose (35.8 %; Fig. 8A), elongated to tubular (59.2 %; Fig. 8B-K) or excentric (5 %; Fig. 8L); diameters averaging 29.2 ± 4.4 µm (overall range 16.5–42.5 µm and range of isolate means 25.4–30.1 µm). Oogonial length 44.8 ± 11.6 µm; tubular viable oogonia (Fig. 8A–J) up to 109.0 µm long, aborted tubular oogonia (Fig. 8M–Q) reaching lengths of 300.0 µm. *Oospores* with a mean diameter of 26.1 ± 3.7 µm (total range 16.0–36.5 µm), plerotic or aplerotic, usually globose (89 %) or less frequently elongated (11 %) assuming the shape of the elongated or excentric oogonium (Fig. 8E–H). Some oogonia with two oospores of which one was usually aborted (Fig. 8J). Oospores with medium-thick walls (2.0 ± 0.6 µm) and a mean oospore wall index of 0.38 ± 0.08; containing either one large ooplast (Fig. 8A–D) or several smaller lipid vacuoles (Fig. 8E–H); abortion high (on. av. 72.3 %; 40–91 %) occurring either before (Fig. 8M–Q) or after the formation of the oospore (Fig. 8F, J–L). Antheridia exclusively paragynous (Fig. 8A–Q) averaging 14.9 ± 3.1 x 10.9 ± 1.7 µm, with shapes ranging from subglobose to club-shaped. Primary hyphae often branching in a mono- or dichasium with the mother hypha ending in a short protruding tip (Fig. 8R–S).

Cultures (Figs 11, 13): *Colonies* of all five *P. tubulina* isolates similar on the four different types of media (Fig. 11); largely submerged with limited felty aerial mycelium around the inoculum plug on all four agar media, uniform on CA and V8A, and irregular to dendroid on PDA; almost no growth on MEA. Temperature–growth relations on V8A are shown in Fig. 13. All isolates with identical cardinal temperatures and similar growth rates at all temperatures. The maximum growth temperature was between 25 and 30 °C. All isolates with slow growth, unable to grow at 30 °C and not resuming growth when plates incubated for 5 d at 30 °C were transferred to

Fig. 7. *Phytophthora tubulina* (CBS 141212 — ex-type), structures formed on V8 agar flooded with soil extract. **A–L, N–S.** Sporangia. **A.** Papillate ovoid. **B.** Papillate obpyriform with laterally attached sporangiophore, on a short lateral hypha. **C.** Papillate mouse-shaped with curved apex. **D.** Papillate subglobose. **E.** Papillate distorted with laterally attached sporangiophore. **F–G.** Papillate obpyriform with beak-like, curved (G) apex. **H.** Bipapillate. **I.** Tripapillate. **J.** Semipapillate, elongated ovoid. **K.** Nonpapillate ovoid with hyphal extension. **L.** Nonpapillate intercalary. **M.** Subglobose catenulate hyphal swellings. **N.** Papillate, ovoid intercalary sporangium and papillate subglobose sporangium. **O.** Nonpapillate ovoid sporangium with short hyphal extension (arrow head), shedding (arrow) from short lateral hypha. **P.** Subglobose to ovoid, papillate sporangium with constriction of sporangiophore. **Q.** Bipapillate detached sporangium. **R.** Direct germination of papillate ovoid sporangium. **S.** Empty obpyriform sporangium after release of zoospores, with beak-like apex, narrow exitpore and conspicuous basal plug. **T.** Branching of sporangiophore into multiple sporangiophores. **U.** Globose to subglobose hyphal swellings with radiating hyphae. Bar A–T = 25 µm, U = 40 µm.

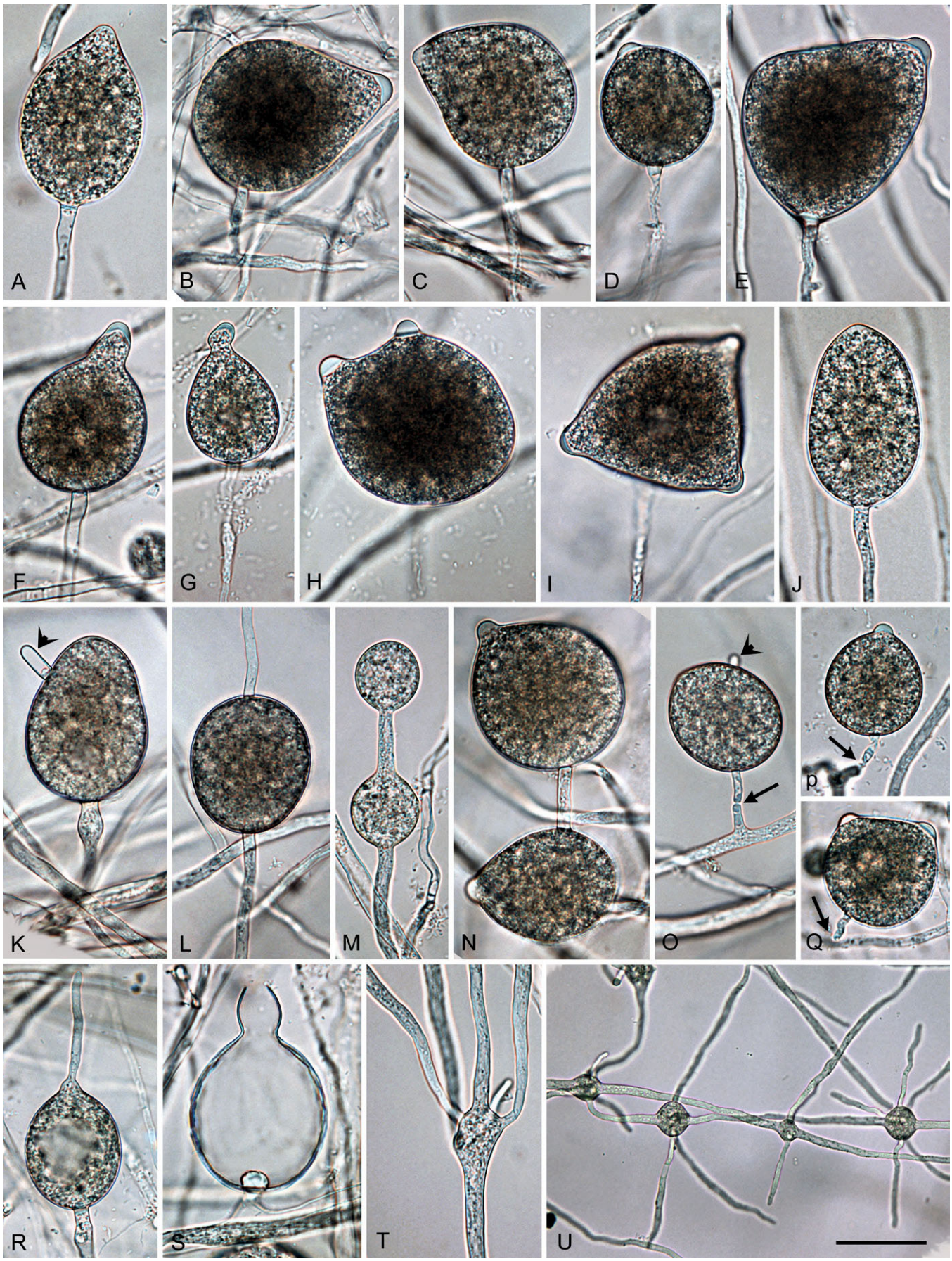
A
B
C
D
E
F
G
H
I
J
K
L
M
N
O
p
Q
R
S
T
U

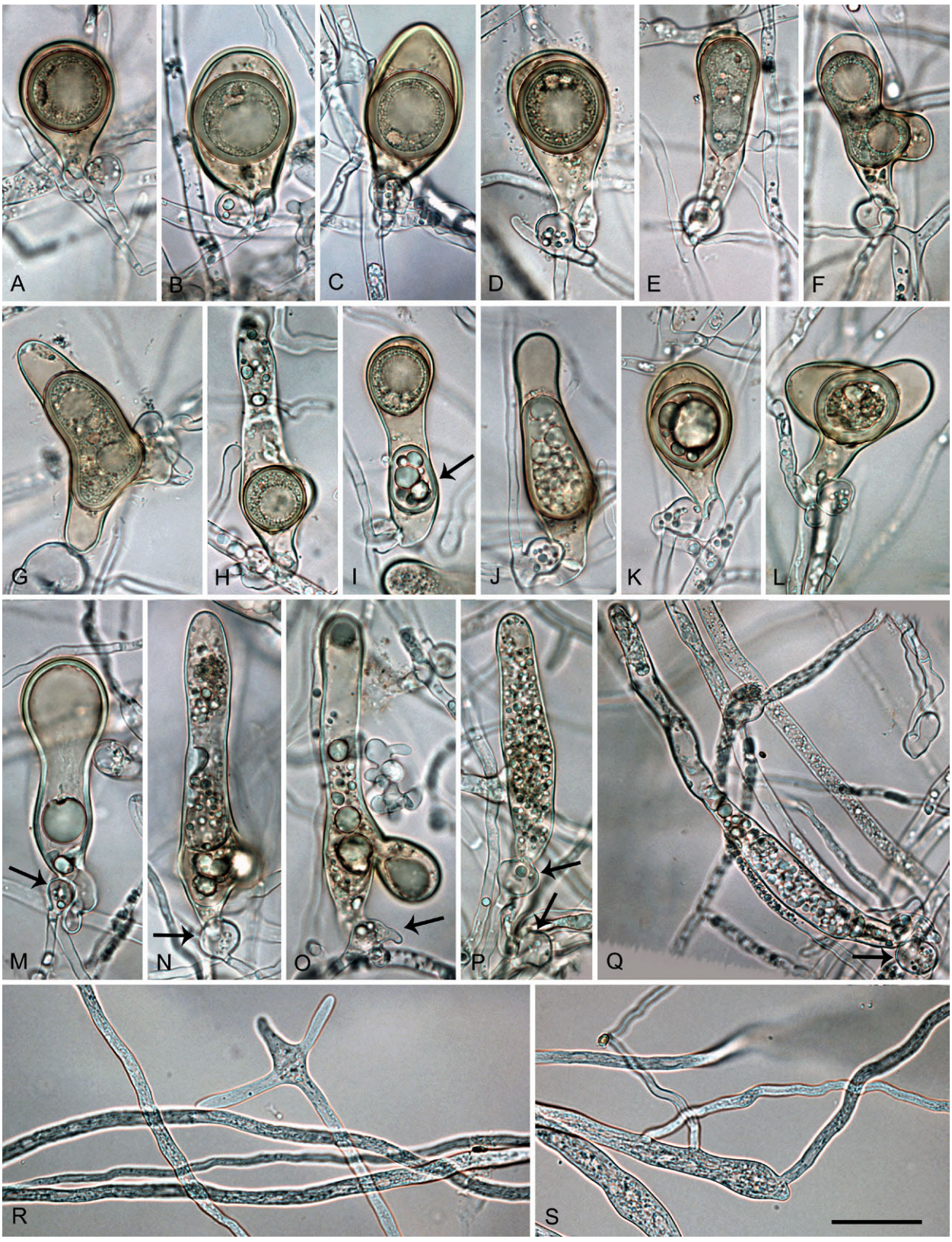

Fig. 8. *Phytophthora tubulina* (CBS 141212 — ex-type), structures formed in solid V8 agar. **A–H.** Mature oogonia with paragynous antheridia, formed in single culture. **A.** Subglobose with tapering base and aplerotic, globose thick-walled oospore. **B–C.** Elongated ellipsoid with tapering bases and aplerotic, globose thick-walled oospores. **D.** Elongated pyriform with tapering base and aplerotic, globose thick-walled oospore. **E.** Elongated tubular with tapering base and plerotic, elongated tubular, thick-walled oospore. **F–G.** Elongated excentric with almost plerotic elongated oospores containing two ooplasts. **H.** Elongated tubular containing a globose, viable thin-walled oospore. **I.** Elongated tubular containing a subglobose, viable thin-walled oospore and a second, ellipsoid aborted oospore (arrow). **J–L.** Oogonia aborted after oospore formation. **J.** Elongated tubular. **K.** Elongated pyriform. **L.** Excentric. **M–Q.** Extremely elongated, tubular oogonia, aborted before oospore formation, with paragynous antheridia (arrows). **R–S.** Primary hyphae branching in a dichasium (R) or monochasium (S) with the mother hypha ending in a short protruding tip. Bar A–S = 25 µm.

20 °C. *Phytophthora tubulina* had a broad growth optimum between 15 and 25 °C with an average radial growth rate of 2.8 ± 1.1 mm/d at 20 °C.

Additional material examined: **Austria:** *Lower Austria*: Dunkelsteiner Forest, isolated from rhizosphere soil of a mature *Fagus sylvatica* tree, Sept. 2010, *T. Jung* (CBS 141213 = TUB2, TUB3, TUB4, TUB5).

Phytophthora tyrrhenica B. Scanu, S.O. Cacciola, Seddaiu, Bakonyi & T. Jung, **sp. nov.**
MycoBank MB819700
(Fig. 9)

Etymology: Name refers to the origin of all known isolates in the Tyrrhenian islands Sardinia and Sicily (tyrrhenica Lat., Tyrrhenian).

Diagnosis: *Phytophthora tyrrhenica* is distinguished from its closest relatives *P. uliginosa* and *P. vulcanica* by the exclusive production of elongated and mostly ellipsoid sporangia, and from *P. vulcanica* also by the absence of amphigynous antheridia.

Type: **Italy:** *Sardinia;* Tergu, isolated from rhizosphere soil of a mature *Quercus ilex* tree, May 2012, *B. Scanu* (CBS H-22984–holotype, dried culture on V8A; CBS 142301 = PH154–ex-type culture). ITS and *cox*1 sequences GenBank KU899188 and KU899343, respectively.

Description: *Sporangia*, *hyphal swellings and chlamydospores* (Fig. 9A–I): *Sporangia* not observed on solid agar but produced abundantly after 24 h in non-sterile soil extract; borne terminally on unbranched sporangiophores, non-caducous, and non-papillate (Fig. 9A–I); ellipsoid to elongated ellipsoid (55.6 %; Fig. 9A, C, I), limoniform to elongated limoniform (18 %; Fig. 9B), ovoid to elongated ovoid (18.8 %; Fig. 9D) and elongated obpyriform (7.6 %); sporangial proliferation usually internal, mainly in a nested (Fig. 9D, F-J) but also extended way (Fig. 9E); dimensions of five isolates 68.4 ± 1.7 x 28.9 ± 1.9 µm (overall range 45.5–110.0 x 16.0–39.5 µm and range of isolate means 66.1–70.0 x 27.5–31.9), with a length/breadth ratio of 2.4–0.18 and a range of isolate means of 2.1–2.57. *Zoospores* discharged through an exit pore 9.0–22.0 µm wide (av. 12.1 ± 2.4 µm) (Fig. 9E–H), limoniform to reniform whilst motile, becoming spherical (av. diam = 14.6 ± 2.3 µm) on encystment; cysts usually germinating directly by forming a hypha but diplanetism also observed in all isolates. Catenulate, intercalary, globose to subglobose or irregular *hyphal swellings* (Fig 9O, P) with an average diameter of 18.6 ± 6.5 µm abundantly produced by most isolates in liquid culture. *Chlamydospores* not observed.

Oogonia, oospores and antheridia (Fig. 9J–N): *Oogonia* produced by all five isolates of *P. tyrrhenica* in single culture on V8A; borne terminally or laterally with globose to subglobose (93.3 %; Fig. 9I–N; P) or slightly excentric (6.7 %; Fig. 9O) shapes, often with a tapering base (52.3 %; Fig. 9I–L, N–P). Oogonial diameters 37.2 ± 3.3 µm (overall range 25.0–39.5 µm and range of isolate means 26.6–44.1 µm). *Oospores* plerotic, globose and usually containing a large ooplast (Fig. 9J–N); mean diameter 33.7 ± 1.3 µm (total range 24.5–40.0 µm), thick walls (av. 2.9 ± 1.5 µm, total range 1.5–4.5 µm), with a mean oospore wall index of 0.41 ± 0.03. Mean oogonial abortion rate low (5 %). *Antheridia* formed terminally or laterally (Fig. 9M), exclusively paragynous, averaging 16.9 ± 4.6 x 12.8 ± 0.13 µm, with shapes ranging from clavate, globose to subglobose.

Cultures (Figs 12–13): *Colonies* uniform with dense-felty to woolly aerial mycelium and regular margin on CA and V8A, and uniform appressed on PDA. All isolates with very limited and irregular growth on MEA (Fig. 12). Temperature-growth relations are shown in Fig. 13. All five isolates included in the growth test with similar growth rates and cardinal temperatures. Maximum growth temperature was 25–30 °C; all isolates resuming growth when plates incubated for 5 d at 30 °C were transferred to 20 °C. Average radial growth rate at the optimum temperature of 20 °C 1.5 ± 0.3 mm/d.

Additional material examined: **Italy:** *Sicily;* Madonie mountains, isolated from rhizosphere soil of mature *Quercus ilex* trees, May 2015, *T. Jung* (TYR1, TYR2, TYR3, TYR4, TYR5, TYR6); *Sardinia;* Tergu, isolated from rhizosphere soil of a mature *Q. ilex* tree, May 2012, *B. Scanu* (PH155); *Sardinia;* Alà dei Sardi, isolated from rhizosphere soil of a mature *Quercus suber* tree, June 2012, *B. Scanu and S. Seddaiu* (CBS 142303 = PH103).

Phytophthora vulcanica T. Jung, M. Horta Jung, Scanu, Bakonyi & Cacciola, **sp. nov.**
MycoBank MB819702
(Fig. 10)

Etymology: Name refers to the origin of all known isolates from volcanic soil (vulcanica Lat., volcanic).

Diagnosis: *Phytophthora vulcanica* differs from its closest relatives *P. uliginosa* and *P. tyrrhenica* by the production of both paragynous and amphigynous antheridia, by its low optimum temperature of 15 °C and by slower growth rates at 15 and 20 °C.

Type: **Italy:** *Sicily;* Mount Etna, isolated from rhizosphere soil of a mature *Fagus sylvatica* tree, May 2013, *T. Jung* (CBS H-22556–holotype, dried culture on V8A; CBS 141216 = X3a–ex-type culture). ITS and *cox*1 sequences GenBank MF036209 and MF036287, respectively.

Description: *Sporangia, hyphal swellings and chlamydospores* (Fig. 10A–I): *Sporangia* not formed on solid agar but produced in non-sterile soil extract; non-caducous and non-papillate with a flat apex (Fig. 10A–E, G); borne terminally, on unbranched sporangiophores or in lax sympodia, or less frequently laterally (Fig. 10D), proliferating internally in both a nested (Fig. 10G, H) and extended way (Fig. 10I). Sporangiophores often branching close to the sporangial base forming lax sympodia (Fig. 10F–G). Sporangial shapes ovoid (52.5 %; Fig. 10A–B, F–G, I), elongated ovoid (14.0 %; Fig. 10C), ellipsoid to elongated ellipsoid (32.5 %; Fig. 10E–F, H) or less frequently limoniform (Fig. 10D), pyriform and obpyriform (1.0 %); dimensions of six isolates 57.3 ± 8.7 x 34.5 ± 4.2 µm (overall range 35.5–81.0 x 22.5–43.0 µm)

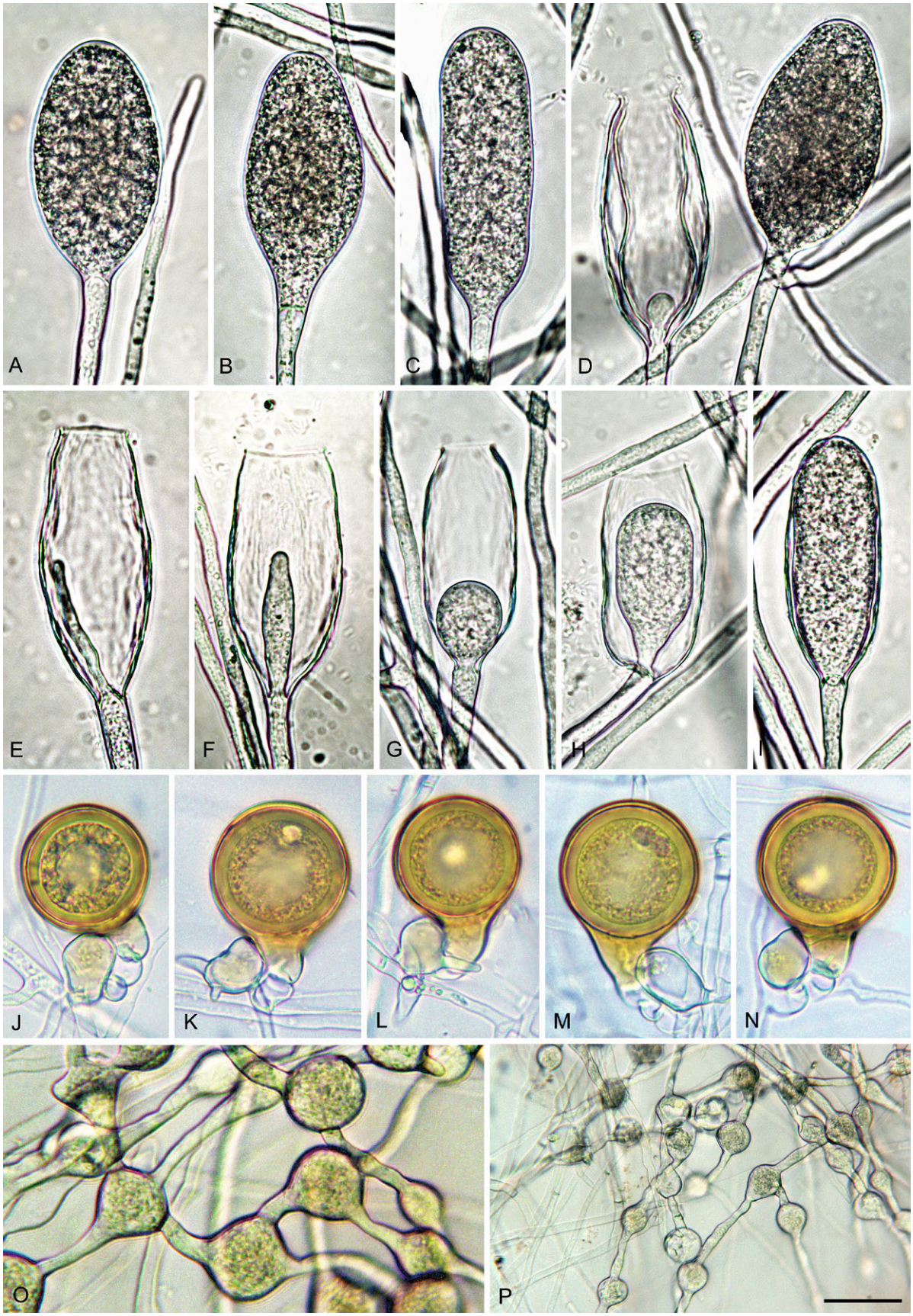

Fig. 9. *Phytophthora tyrrhenica* (CBS 142301 — ex-type). **A–I.** Sporangia formed on V8 agar (V8A) flooded with soil extract. **A–D.** Nonpapillate with flat apex. **A.** Ellipsoid. **B.** Limoniform with tapering base. **C.** Elongated ellipsoid. **D.** Mature ovoid (right) and empty with wide exit pore and internal nested proliferation (left). **E–I.** Empty with wide exit pores and internal extended (E) or internal nested proliferation (F–I). **J–N.** Mature, golden-brown, smooth-walled, globose oogonia formed in single culture in V8A, containing thick-walled plerotic oospores with big ooplasts, with paragynous antheridia. **K–L.** Antheridia with finger-like hyphal extensions. **O–P.** Globose, limoniform and angular catenulate hyphal swellings formed on V8A flooded with soil extract. Bar A–O = 25 µm, P = 50 µm.

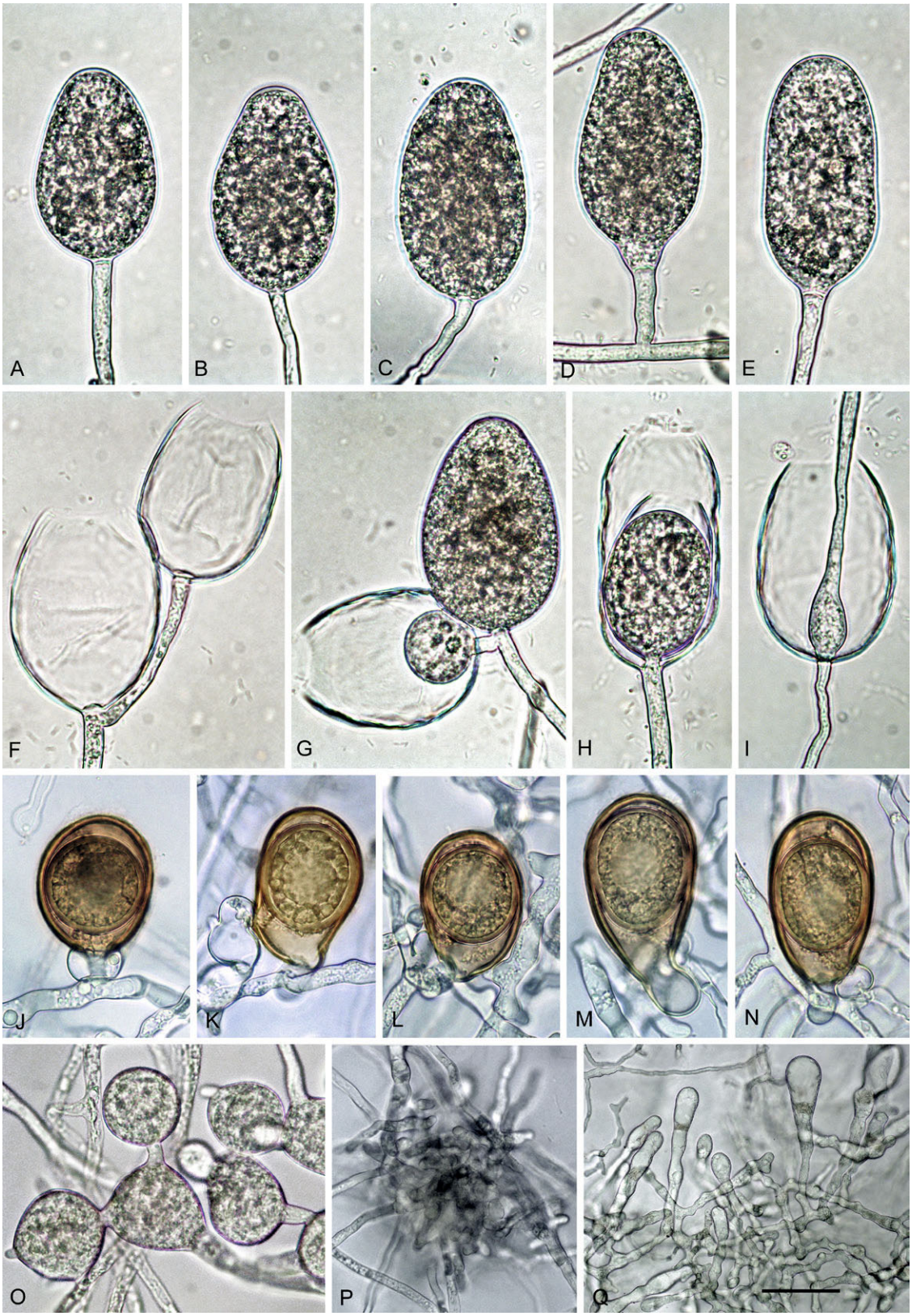

Fig. 10. *Phytophthora vulcanica* (CBS 141216 — ex-type). **A–I.** Sporangia formed on V8 agar (V8A) flooded with soil extract. **A–E.** Nonpapillate with flat apex. **A–B.** Ovoid. **C.** Elongated ovoid. **D.** Limoniform, on short lateral hypha. **E.** Elongated ellipsoid. **F.** Empty sporangia after release of zoospores through wide exitpores, showing external proliferation. **G.** Empty sporangium with both internal nested proliferation (arrow) and external proliferation forming a mature ovoid sporangium. **H.** Empty, elongated ellipsoid sporangium with internal nested proliferation. **I.** Empty ovoid sporangium with internal extended proliferation. **J–N.** Mature, golden-brown oogonia formed in single culture in V8A, with medium thick-walled oospores. **J.** Subglobose with aplerotic globose oospore and amphigynous antheridium. **K.** Elongated, slightly excentric with aplerotic subglobose oospore and paragynous antheridium. **L.** Obovoid with aplerotic globose oospore and paragynous antheridium. **M.** Elongated ellipsoid with aplerotic ellipsoid oospore and paragynous antheridium. **N.** Elongated pyriform with plerotic ellipsoid oospore. **O.** Globose and triangular, catenulate hyphal swellings. **P.** Dense hyphal aggregation. **Q.** Tubular to elongated club-shaped hyphae. Bar A–O = 25 µm, P–Q = 40 µm.

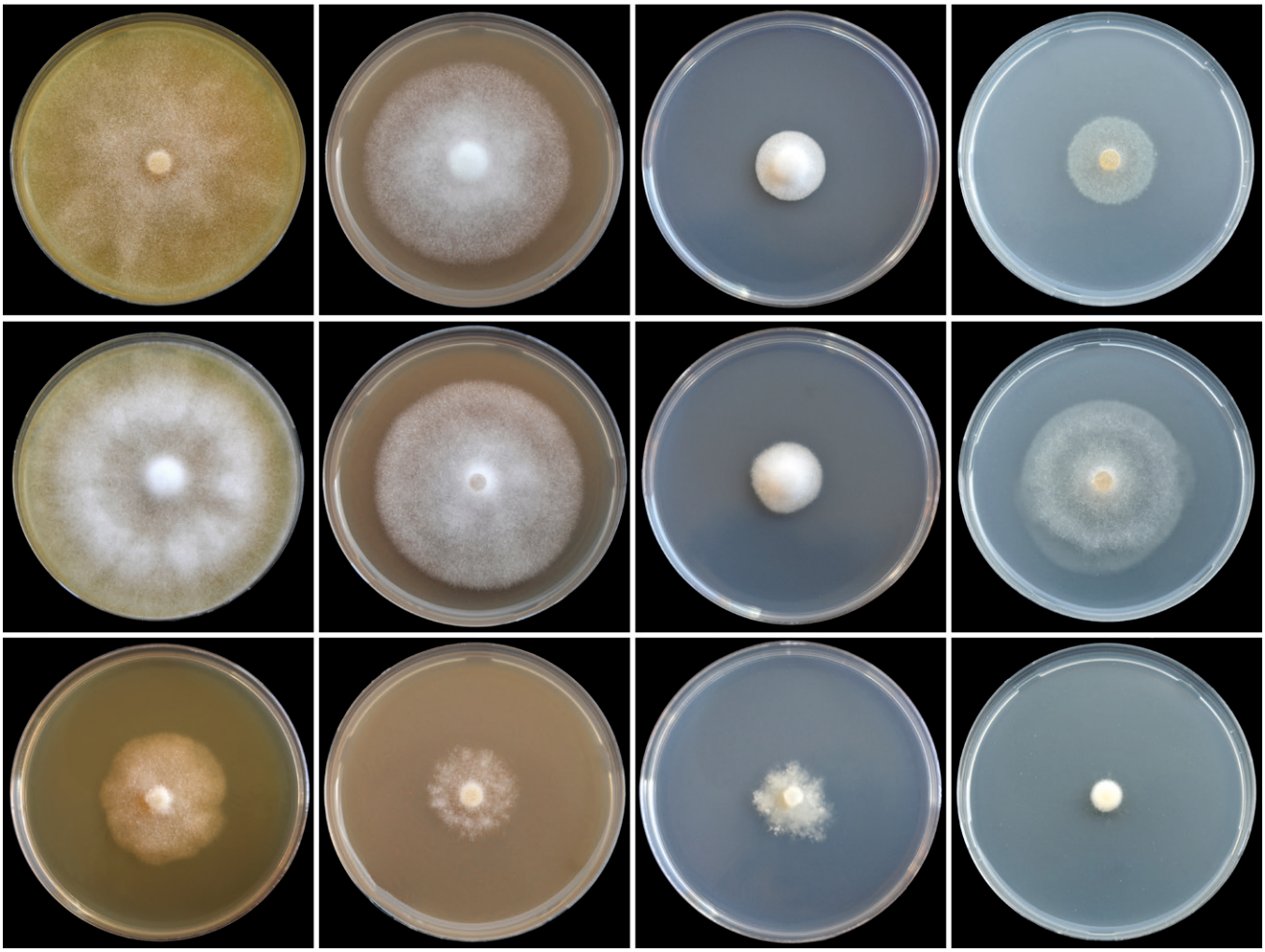

Fig. 11. Colony morphology of *Phytophthora castanetorum* (CBS 142299), *P. quercina* (Beja 5) and *P. tubulina* (CBS 141212) (from top to bottom) after 10 d growth at 20 ºC on carrot agar, V8 agar, potato-dextrose agar and malt extract agar (from left to right).

with a range of isolate means of 53.6–61.0 x 31.8–36.4 µm, and a length/breadth ratio of 1.67 ± 0.22 (range of isolate means 1.58–1.72). *Zoospores* of *P. vulcanica* discharged through wide exit pores averaging 17.0 ± 3.0 µm (12.0–25.0 µm), limoniform to reniform whilst motile, becoming spherical (av. diam = 10.0 ± 1.2 µm) on encystment; cysts usually germinating directly but diplanetism also observed in all isolates. *Swellings* formed on sporangiophores by all isolates, subglobose, angular or irregular, often catenulate (Fig. 10O), with an average diameter of 21.1 ± 5.5 µm. *Chlamydospores* not observed.

Oogonia, oospores, antheridia and hyphae (Fig. 10J–Q): *Oogonia* produced by all five isolates on V8A in single culture; borne terminally or laterally, with smooth walls and often tapering (37.3 %; Fig. 10L–N) or curved bases (7.2 %; Fig. 10M); elongated, ellipsoid to pyriform or excentric (on av. 65.7 %; Fig. 10K–N) or less frequently globose to subglobose (34.3 %; Fig. 10J), turning golden-brown during ageing (Fig. 10J–N); mean 35.8 ± 3.6 µm diam. with an overall range of 23.0–46.0 µm and isolate means ranging from 33.6–36.5 µm. *Oospores* with a mean diameter of 30.5 ± 3.2 µm (total range 20.0–38.0 µm), aplerotic (72.7 %) or less frequently plerotic (27.3 %), containing a large ooplast (Fig. 10J–N); medium thick-walled (2.4 ± 0.4 µm), with a mean oospore wall index of 0.40 ± 0.06. High oogonial abortion rate in most isolates (av. 52.8 %; 0–80 %). *Antheridia* 16.3 ± 3.1 x 12.6 ± 2.3 µm, predominantly paragynous (95.3 %; Fig. 10K–N) but few amphigynous antheridia observed in all isolates (4.7 %; Fig. 10J). *Hyphal aggregations* regularly formed by all isolates (Fig. 10P). *Hyphae* often inflated-tubular to club-shaped (Fig. 10Q).

Cultures (Figs 12–13): *Colonies* of all *P. vulcanica* isolates uniform felty on CA and V8A , with irregular margins on CA and dome-shaped with regular margins on V8A; very limited and irregular growth on PDA and MEA (Fig. 12). Temperature–growth relations on V8A are shown in Fig. 13. All isolates with very slow growth and similar growth rates at all temperatures; maximum growth temperature between 25 and 30 °C. Isolates with no growth when plates incubated for 5 d at 30 °C were transferred to 20 °C. Average radial growth rate at the optimum temperature of 15 °C 0.7 ± 0.1 mm/d.

Additional material examined: **Italy:** *Sicily;* Mount Etna, isolated from rhizosphere soil of mature *F. sylvatica* trees, May 2013, T. Jung (CBS 141217 = X3b, X3c, X3d, X3e).

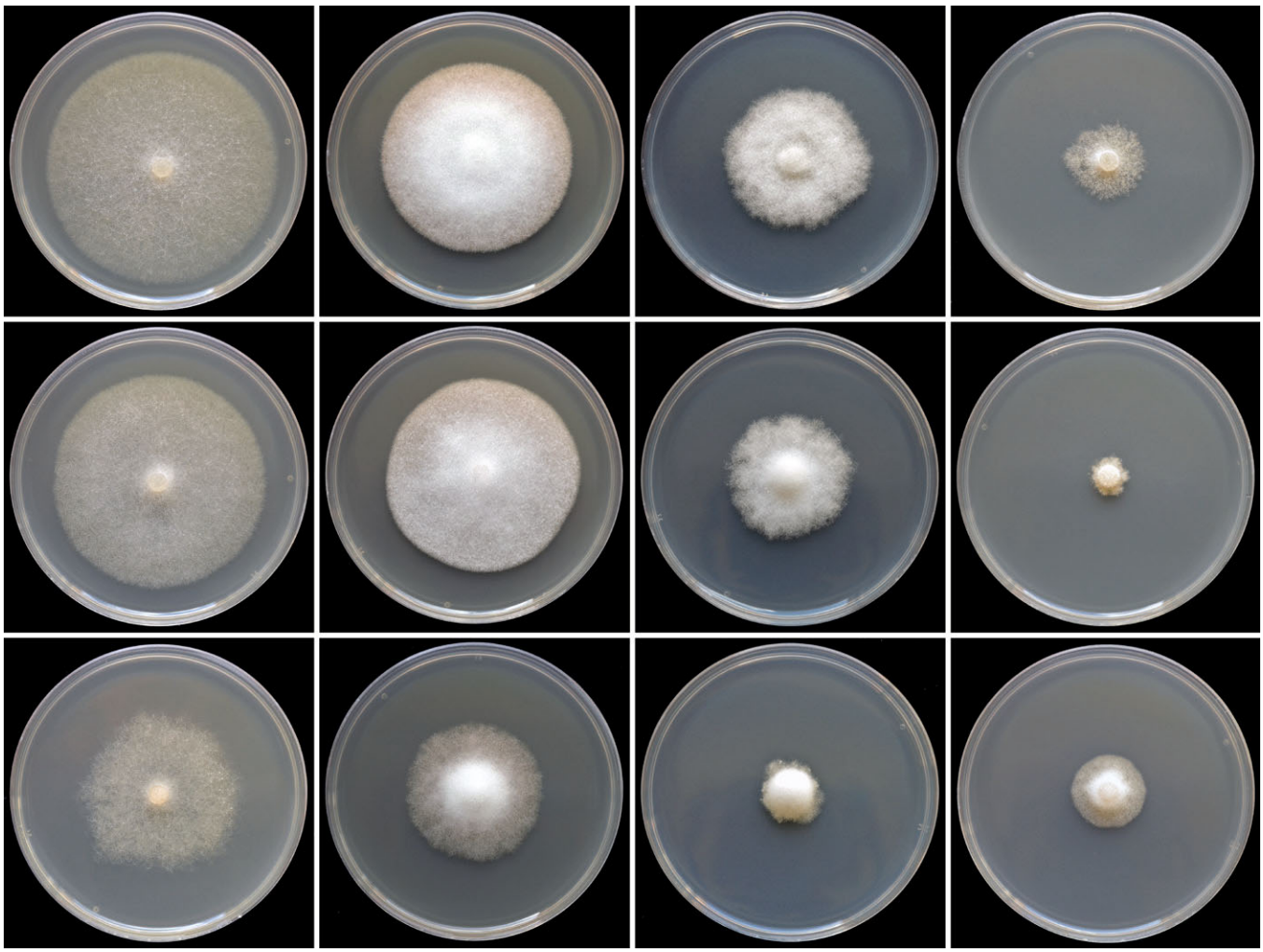

Fig. 12. Colony morphology of *Phytophthora tyrrhenica* from Sardinia (CBS 142301), *P. tyrrhenica* from Sicily (CBS 142302) and *P. vulcanica* (CBS 141216) (from top to bottom) after 15 d growth at 20ºC on carrot agar, V8 agar, potato-dextrose agar and malt extract agar (from left to right).

DISCUSSION

Four new cryptic *Phytophthora* species recently isolated from *Fagaceae* trees in forest stands in Austria, Italy, and Portugal were characterized. Phylogenetic analyses of the DNA sequence data for three nuclear (ITS, Btub and HSP90) and two mitochondrial (*cox*1 and NADH1) gene regions together with detailed morphological and physiological studies allowed the description of these four taxa as *P. castanetorum*, *P. tubulina*, *P. tyrrhenica,* and *P. vulcanica*.

Multigene phylogenetic analyses demonstrated that *P. castanetorum* and *P. tubulina* are distinct species closely related to *P. quercina*. In previous studies, the phylogenetic position of *P. quercina* was ambiguous and, depending on the gene regions analysed, this species loosely clustered with Clade 3 (ITS; Cooke *et al.* 2000), Clade 4 (seven nuclear loci; Blair *et al.* 2008), Clade 5 (four mitochondrial loci; Martin *et al.* 2014), and Clade 1 (seven nuclear loci; Martin *et al.* 2014). Due to the inclusion of *P. castanetorum*, *P. tubulina* and the three taxa *P.* sp. ohioensis, *P. versiformis* and *P.* sp. versiformis-like in the phylogenetic analyses of both a four-locus (ITS, Btub, HSP90, NADH1) and a nuclear three-locus (ITS, Btub, HSP90) dataset in this work the phylogenetic position of the *P. quercina* clade within *Phytophthora* could be resolved. *Phytophthora quercina*, *P. castanetorum*, *P. tubulina*, *P.* sp. ohioensis, *P. versiformis* and *P.* sp. versiformis-like, formed a fully supported monophyletic group. Due to the unique phylogenetic position of *P. lilii*, which was confirmed in both the phylogenetic analysis of the three-locus dataset here, and a new expanded phylogeny of *Phytophthora* with more than 150 taxa included (Yang *et al*. 2017), Rahman *et al.* (2015) proposed that *P. lilii* constituted an eleventh *Phytophthora* clade. Consequently, the *P. lilii* clade and the *P. quercina* clade are named here as Clades 11 and 12, respectively.

All Clade 12 species in Europe and North America are associated with *Fagaceae*. *Phytophthora quercina* is involved in decline syndromes of natural and planted *Quercus* stands (*Q. cerris*, *Q. coccinea*, *Q. faginea*, *Q. ilex*, *Q. palustris*, *Q. petraea*, *Q. pubescens*, *Q. pyrenaica*, *Q. robur*, *Q. rubra*, *Q. suber*, and *Q. vulcanica*) across Europe causing a progressive destruction of fine root systems, which predisposes affected oaks to climatic extremes and secondary pathogens and pests (Jung *et al.* 1999, 2000, 2013, 2016, Balci & Halmschlager 2003a, b, Perez-Sierra *et al.* 2013). Interestingly, *P.* sp. ohioensis and *P.* sp.

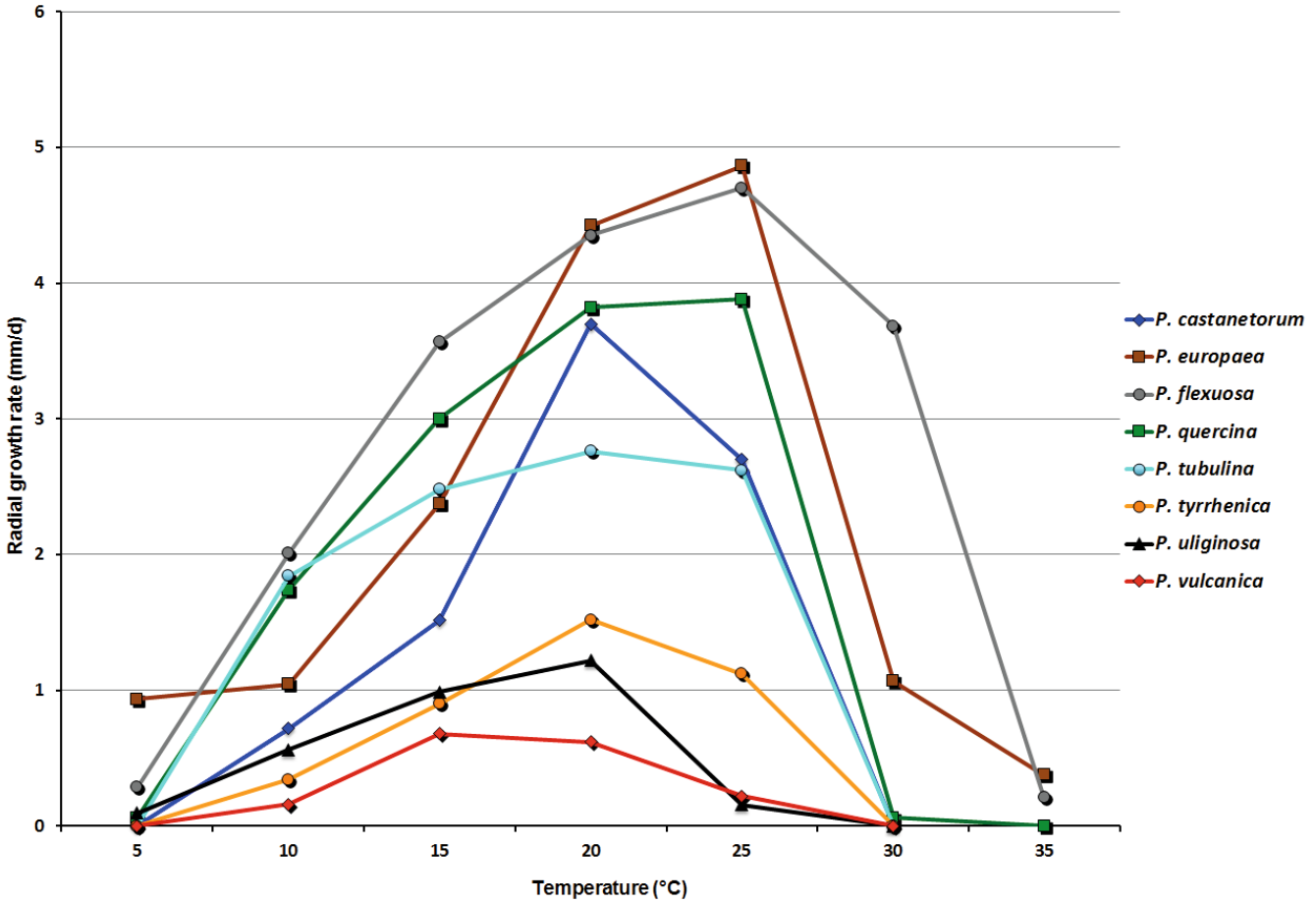

Fig. 13. Mean radial growth rates of *Phytophthora castanetorum* (6 isolates), *P. tubulina* (5 isolates), *P. quercina* (5 isolates), *P. tyrrhenica* (5 isolates), *P. vulcanica* (5 isolates), *P. uliginosa* (2 isolates), *P. europaea* (5 isolates) and *P. flexuosa* (3 isolates) on V8 agar at different temperatures.

quercina-like were also found associated with oak forests in the USA, the latter taxon with *Q. ellipsoides* and *Q. rubra* in Minnesota and Wisconsin, respectively (Balci *et al.* 2007), and *P.* sp. ohioensis with declining *Q. alba* in southern Ohio (Balci *et al.* 2010). *Phytophthora* sp. quercina-like was also recovered from oak seedlings in woody ornamental nurseries in Minnesota (Schwingle *et al.* 2007). *Phytophthora castanetorum* and *P. tubulina* were isolated from the other two genera of *Fagaceae* in Europe, *Castanea* and *Fagus*, respectively. Interestingly, in Australia, which lacks any native *Fagaceae, P. versiformis* and *P.* sp. versiformis-like were both frequently isolated from the rhizosphere of a *Myrtaceae* tree (*Corymbia calophylla*) in remnant bushland, parks and gardens in the southwest of Western Australia (Barber *et al.* 2013, Paap *et al.* 2017). In a metagenomic *Phytophthora* survey of rhizosphere soils, *P. versiformis* was detected in more than 10 % of the 640 sites sampled across Australia, and due to its consistent association with native vegetation it was considered as a native species (Burgess *et al*. 2017).

Both *P. castanetorum* and *P. tubulina* share basic phenotypic features with their closest relative *P. quercina*, such as the homothallic breeding system, production of elongated oogonia and persistent papillate sporangia, sympodial hyphal branching with the mother hypha ending with a protruding tip, slow growth in culture and uniform woolly colony growth patterns, but differed in a number of characters (Table 2). *Phytophthora castanetorum* and *P. tubulina* produce a low proportion of semipapillate and nonpapillate sporangia, whereas sporangia of *P. quercina* are exclusively papillate. *Phytophthora tubulina* also forms markedly longer sporangia than the other two species and partially extremely elongated, often tubular oogonia with high oospore abortion rates, suggesting genetic instability. *Phytophthora castanetorum* differed from the other two species in the regular production of chlamydospores, and by having on average higher oogonial diameters and a higher percentage of elongated oogonia. *Phytophthora quercina* grew faster at all temperatures tested and had a higher optimum temperature for growth than *P. castanetorum* and *P. tubulina* (25 vs 20 °C).

Concerning *P. tyrrhenica* and *P. vulcanica*, multigene phylogenetic analyses placed both species in Clade 7a (Cooke *et al.* 2000, Blair *et al.* 2008), with *P. tyrrhenica* forming a sister clade to *P. uliginosa* and *P. vulcanica* residing in a basal position of the subclade. Recently, six new *Phytophthora* species from Clade 7a occurring in natural ecosystems in Taiwan were described and two other new Clade 7a taxa were informally designated (Jung *et al.* 2017a, b) expanding the number of extant taxa in

Clade 7a to 16. Besides the new Taiwanese species, Clade 7a contains several important plant pathogens like the multivorous *P.* x*cambivora* and the host-specific *P. fragariae*, *P. rubi*, *P. uniformis*, *P.* x*alni* and *P.* x*multiformis*, but also cryptic species such as *P. europaea* and *P. uliginosa* (Jung *et al.* 2002, 2017b). Their scattered distribution and putative host specialization also suggests a cryptic nature for both *P. tyrrhenica* and *P. vulcanica*. Morphologically these two species are similar to their closest relative *P. uliginosa* (Table 2). The main distinguishing characters are the exclusive production of elongated and mostly ellipsoid sporangia in *P. tyrrhenica*, the occurrence of both amphigynous and paragynous antheridia in *P. vulcanica* and the average largest oogonial and oospore diameters in *P. uliginosa*. All three species show similar slow growth rates, but differ in their optimum temperatures for growth and their growth rates at 25 °C, with *P. vulcanica* being the most psychrophilic and *P. tyrrhenica* the most thermophilic species.

The lack of previous records of all four new species from other continents, their apparent absence from European nurseries (Jung *et al.* 2016) and their exclusive occurrence in natural and semi-natural *Fagaceae* forest ecosystems in Europe indicate that *P. castanetorum*, *P. tubulina*, *P. tyrrhenica,* and *P. vulcanica* may be endemic to Europe or were introduced in historic times and have evolved *in situ*. These hypotheses are also supported by the intraspecific variability in both mitochondrial and nuclear DNA, observed particularly in *P. castanetorum* and *P. tyrrhenica*. This is in contrast to genetically uniform populations of recently introduced *Phytophthora* species which originated from relatively small and genetically impoverished founder populations (Goodwin *et al*. 1992). One well-known example is *P. cinnamomi*, whose global invasion was mainly achieved by the clonal spread of two genotypes from the A2 mating type (Oudemans & Coffey 1991, Dobrowolski *et al.* 2003). The other two new species, *P. tubulina* and *P. vulcanica*, were monomorphic across all five loci examined resulting in two clonal population structures. However, this is most likely due to their scattered distribution and the origin of all isolates per species from one site. More isolates from different geographic locations are needed to confirm the endemic origin also for these two species. That the four new species and their closest European relatives *P. quercina*, *P. europaea* and *P. uliginosa* are all exclusively associated with *Fagaceae* suggests sympatric species radiation driven by the adaptation to different genera of *Fagaceae* in Europe.

All four new species from *Fagaceae* forests showed a low maximum temperature for growth and an optimum temperature between 15 °C and 25 °C. This is similar to that of other possibly endemic low-temperature *Phytophthora* species such as *P. ilicis*, *P. pseudosyringae*, *P. psychrophila,* and *P. quercina* (Jung *et al.* 1999, 2002, Pérez-Sierra *et al.* 2013, Scanu *et al.* 2014b, Scanu & Webber 2016). All four new species are homothallic, with a high oospore wall index (range 0.4–0.5) enabling them to survive both the long hot and dry summers typical of Mediterranean regions (*P. castanetorum*, *P. tyrrhenica,* and *P. vulcanica*) and cold winters in Austria (*P. tubulina*), on Mount Etna (*P. vulcanica*), and in the Gennargentu Mountain and Serra da Estrela (*P. castanetorum*).

While *P. vulcanica* was isolated alone and from relatively healthy beech trees, *P. castanetorum*, *P. tyrrhenica,* and *P. tubulina* co-occurred with other *Phytophthora* species in the rhizosphere of declining trees. Infections by multiple *Phytophthora* species have been previously reported in *Fagaceae* (Jung 2009, Jung *et al.* 2013, Pérez-Sierra *et al.* 2013, Scanu *et al.* 2015). Because of their co-occurrence with aggressive pathogens of chestnut, beech, and oaks, such as *P.* x*cambivora*, *P. cinnamomi*, and *P. plurivora*, it is not possible to establish whether the new species were directly involved in the decline of *Fagaceae* in Europe. Pathogenicity tests, however, showed that all four new species are able to damage the roots of young seedlings of their respective hosts: beech, chestnut, and oak. In comparison to the aggressiveness of invasive *Phytophthora* species co-occurring with them, they must nevertheless be considered as relatively weak pathogens. For example, in a soil infestation trial during this study, *P.* x*cambivora* caused much higher mortality of chestnut seedlings than *P. castanetorum* (90 % vs <20 %). In addition, *P. tubulina* and *P. vulcanica* killed only a low proportion of beech seedlings in artificially infested soil whereas the mortality rate caused by *P.* x*cambivora* exceeded 50 %. The only exception was *P. tyrrhenica*, which showed considerable aggressiveness to *Quercus ilex* seedlings, although less virulent than *P. cinnamomi*. Their relatively low aggressiveness to their native *Fagaceae* hosts supports the endemism hypothesis.

The continuously increasing diversity of both invasive and potentially endemic *Phytophthora* species in Mediterranean *Fagaceae* forests (Scanu *et al.* 2010, Jung *et al.* 2013, Peréz-Sierra *et al.* 2013; this study) necessitates future studies to address the ecology of these cryptic species in *Fagaceae* ecosystems. Most plausibly, they live as fine root “nibblers” as demonstrated for *P. quercina* (Jung *et al.* 1999, 2000, Peréz-Sierra *et al.* 2013) causing a slow chronic decline which in interaction with climatic extremes and secondary pathogens and pests might cause episodic dieback and mortality (Jung *et al.* 2000, Jung 2009, Peréz-Sierra *et al.* 2013). A similar life-style was also suggested for the potentially native *P. arenaria* and *P. constricta* in Western Australia (Rea *et al.* 2011). In addition, the four new species may act as damping-off pathogens affecting seedling recruitment, as reported previously for other *Phytophthora* species (Cohen & Coffey 1986, Simamora *et al.* 2015). This is particularly plausible for *P. tyrrhenica* considering the high susceptibility of germinating *Q. ilex* acorns to *Phytophthora*, due to the poor suberisation and lignification of tissues and restricted allocation of defence compounds (Herms & Mattson, 1992, Martín-García *et al.* 2015, B. Scanu & G. Hardy, unpubl.). However, these hypotheses need to be further investigated, for both the new species described here and other *Phytophthora* species occurring in *Fagaceae* forest ecosystems. It would also be important to test whether co-infections of trees by endemic and invasive *Phytophthora* species are causing synergistic or antagonistic interactions. In a recent study conducted by Corcobado *et al.* (2017), no synergistic interaction was found when *Q. ilex* seedlings were grown in soil artificially infested with two different *Phytophthora* species. On the contrary, mortality of *Q. ilex* seedlings was delayed if the less virulent and potentially endemic European pathogens *P.*

gonapodyides and *P. quercina* were inoculated prior to the aggressive invasive *P. cinnamomi* (Corcobado *et al.* 2017), most likely due to the priming of induced resistance. The putatively endemic, new species may also have a beneficial effect in maintaining plant diversity in these ecosystems. In the kwongan shrublands in Western Australia, the putatively endemic *P. arenaria* and *P. constricta* (Rea *et al.* 2011) can affect the growth of non-mycorrhizal plants while they do not affect co-occurring ectomycorrhizal (ECM) ones, thus conferring an advantage to ECM species in terms of accessing scarce phosphorus resources (Albornoz *et al.* 2016). Consequently, the occurrence of *P. castanetorum* and *P. tyrrhenica* in old impoverished soils in Portugal and Sardinia that are particularly low in phosphorus might suggest a similar ecological contribution to the maintenance of highly diverse ecosystems by reducing differences in competitiveness between plant species of contrasting nutrient-acquisition strategies.

With the advent of molecular-based techniques, the systematics and evolutionary understanding of the genus *Phytophthora* has advanced and the detection and description of new *Phytophthora* species have become a priority. However, more studies on pathogen-host-environment interactions are urgently required to increase our understanding of the ecology of cryptic endemic *Phytophthora* species in natural forest ecosystems.

ACKNOWLEDGEMENTS

We are grateful to the Portuguese Science and Technology Foundation (FCT) for co-financing with Portuguese national funds the European BiodivERsA project RESIPATH: Responses of European Forests and Society to Invasive Pathogens (BIODIVERSA/0002/2012), and to the Czech Ministry for Education, Youth and Sports and the European Regional Development Fund for financing the Project Phytophthora Research Centre Reg. No. CZ.02.1.01/0.0/0.0/15_003/0000453. Fieldwork in Portugal had logistic support from the Institute for the Conservation of Nature and Forestry (ICNF). DNA sequencing was partly supported by the Hungarian Scientific Research Fund (OTKA) grant K101914. This work has also received funding from the European Union's Horizon 2020 research and innovation programme under grant agreement No 635646, POnTE (Pest Organisms Threatening Europe). Part of this study was also financially supported by the Sardinian Regional Government (Accordo di collaborazione tecnico-scientifica tra la Regione autonoma della Sardegna, Assessorato della difesa dell'ambiente, e il Dipartimento di Agraria dell'Università degli studi di Sassari per la realizzazione di attività di ricerca e sviluppo nel campo della pianificazione e programmazione della tutela fitosanitaria delle foreste sarde). We thank Treena Burgess (Murdoch University, Perth) for assistance with Figs 7 and 8.

REFERENCES

Abad GZ, Ivors KL, Gallup CA, Abad JA, Shew HD (2011) Morphological and molecular characterization of *Phytophthora glovera* sp. nov. from tobacco in Brazil. *Mycologia* **103**: 341–350.

Abad GZ, Abad JA, Cacciola SO, Pane A, Faedda R, *et al.* (2014) *Phytophthora niederhauserii* sp. nov., a polyphagous species associated with ornamentals, fruit trees and native plants in 13 countries. *Mycologia* **106**: 431–447.

Albornoz FE, Burgess TI, Lambers H, Etchells H, Laliberté E (2016) Native soil-borne pathogens equalise differences in competitive ability between plants of contrasting nutrient-acquisition strategies. *Journal of Ecology* **105**: 549–557.

Balci Y, Balci S, Eggers J, MacDonald WL, Juzwik J, *et al*. (2007) *Phytophthora* spp. associated with forest soils in Eastern and North-Central U.S. oak ecosystems. *Plant Disease* **91**: 705–710.

Balci Y, Halmschlager E (2003a) Incidence of *Phytophthora* species in oak forests in Austria and their possible involvement in oak decline. *Forest Pathology* **33**: 157–174.

Balci Y, Halmschlager E (2003b) *Phytophthora* species in oak ecosystems in Turkey and their association with declining oak trees. *Plant Pathology* **52**: 694–702.

Balci Y, Long RP, Mansfield M, Balser D, MacDonald WL (2010) Involvement of *Phytophthora* species in white oak (*Quercus alba*) decline in southern Ohio. *Forest Pathology* **40**: 430–442.

Barber P, Paap T, Burgess T, Dunstan W, Hardy GSJ (2013) A diverse range of *Phytophthora* species are associated with dying urban trees. *Urban Forestry and Urban Greening* **12**: 569–575.

Bezuidenhout CM, Denman S, Kirk SA, Botha WJ, Mostert L, McLeod A (2010) *Phytophthora* taxa associated with cultivated *Agathosma*, with emphasis on the *P. citricola* complex and *P. capensis* sp. nov. *Persoonia* **25**: 32–49.

Blair JE, Coffey MD, Park S, Geiser DM, Kang S (2008) A multilocus phylogeny for *Phytophthora* utilizing markers derived from complete genome sequences. *Fungal Genetics and Biology* **45**: 266–277.

Brazee NJ, Wick RL, Hulvey JP (2016) *Phytophthora* species recovered from the Connecticut River Valley in Massachusetts, USA. *Mycologia* **108**: 6–19.

Burgess TI, White D, McDougall KM, Garnas J, Dunstan WA, *et al.* (2017) Distribution and diversity of *Phytophthora* across Australia. *Pacific Conservation Biology* **23**: 1–13.

Cohen Y, Coffey MD (1986) Systemic fungicides and the control of Oomycetes. *Annual Review of Phytopathology* **24**: 311–338.

Cooke DEL, Drenth A, Duncan JM, Wagels G, Brasier CM (2000) A molecular phylogeny of *Phytophthora* and related oomycetes. *Fungal Genetic and Biology* **30**: 17–32.

Corcobado T, Miranda-Torres JJ, Martìn-Garcìa J, Jung T, Solla A (2017) Early survival of *Quercus ilex* subspecies from different populations after infections and co-infections by multiple *Phytophthora* species. *Plant Pathology* **76**: 792–804.

Dick MW (1990) *Keys to Pythium*. Reading: University of Reading Press.

Dobrowolski MP, Tommerup IC, Blakeman HD (2003) Non-mendelian inheritance revealed in a genetic analysis of sexual progeny of *Phytophthora cinnamomi* with microsatellite markers. *Fungal Genetics and Biology* **35**: 197–212.

Erwin DC, Ribeiro OK (1996) *Phytophthora Diseases Worldwide*. St Paul, MN: American Phytopathological Society Press.

Gallegly ME, Hong C (2008) *Phytophthora*: *identifying species by morphology and DNA fingerprints*. St Paul, MN: American Phytopathological Society Press.

Goodwin SB, Spielman LJ, Matuszak JM, Bergeron SN, Fry WE (1992) Clonal diversity and genetic differentiation of *Phytophthora infestans* populations in northern and central Mexico. *Phytopathology* **82**: 955–61.

Hansen EM, Reeser PW, Davidson JM, Garbelotto M, Ivors K,

Douhan L, Rizzo DM (2003) *Phytophthora nemorosa*, a new species causing cankers and leaf blight of forest trees in California and Oregon, U.S.A. *Mycotaxon* **88**: 129–138.

Hansen EM, Wilcox WF, Reeser PW, Sutton W (2009) *Phytophthora rosacearum* and *P. sansomeana*, new species segregated from the *Phytophthora megasperma* ''complex''. *Mycologia* **101**: 129–135.

Henricot B, Pérez-Sierra A, Jung T (2014) *Phytophthora pachypleura* sp. nov., a new species causing root rot of *Aucuba japonica* and other ornamentals in the United Kingdom. *Plant Pathology* **63**: 1095–1109.

Herms DA, Mattson WJ (1992) The dilemma of plants to grow or defend. *Quarterly Review of Biology* **67**: 283–335.

Huelsenbeck JP, Ronquist F (2001) MrBayes: Bayesian inference of phylogeny. *Bioinformatics* **17**: 754–755.

Husson C, Aguayo J, Revellin C, Frey P, Ioos R, *et al*. (2015) Evidence for homoploid speciation in *Phytophthora alni* supports taxonomic reclassification in this species complex. *Fungal Genetics and Biology* **77**: 12–21.

Ilieva E, Man In 't Veld WA, Veenbaas-Rijks W, Pieters R (1998) *Phytophthora multivesiculata*, a new species causing rot in Cymbidium. *European Journal of Plant Pathology* **104**: 677–684.

Jee H-J, Cho W-D, Kim W-G (1997) *Phytophthora* diseases of apple in Korea: 2. Occurrence of an unusual fruit rot caused by *P. cactorum* and *P. cambivora*. *Korean Journal Plant Pathology* **13**: 145–151.

Józsa A, Bakonyi J, Belbahri L, Nagy ZÁ, Szigethy A, Bohár G, *et al*. (2010) A new species of *Phytophthora* reported to cause root and collar rot of common boxwood, Nordmann fir and Port Orford cedar in Hungary. *Plant Pathology* **59**: 1166–1167.

Jung T (2009) Beech decline in Central Europe driven by the interaction between *Phytophthora* infections and climatic extremes. *Forest Pathology* **39**: 73–94.

Jung T, Blaschke H, Neumann P (1996) Isolation, identification and pathogenicity of *Phytophthora* species from declining oak stands. *European Journal of Forest Pathology* **26**: 253–272.

Jung T, Blaschke H, Oßwald W (2000) Involvement of soilborne *Phytophthora* species in Central European oak decline and the effect of site factors on the disease. *Plant Pathology* **49**: 706–718.

Jung T, Chang TT, Bakonyi J, Seress D, Pérez-Sierra A, *et al*. (2017a) Diversity of *Phytophthora* species in natural ecosystems of Taiwan and association with disease symptoms. *Plant Pathology* **66**: 194–211.

Jung T, Cooke DEL, Blaschke H, Duncan JM, Oßwald W (1999) *Phytophthora quercina* sp. nov., causing root rot of European oaks. *Mycological Research* **103**: 785–798.

Jung T, Hansen EM, Winton L, Oßwald W, Delatour C (2002) Three new species of *Phytophthora* from European oak forests. *Mycological Research* **106**: 397–411.

Jung T, Horta Jung M, Scanu B, Seress D, Kovács GM *et al*. (2017b) Six new *Phytophthora* species from ITS Clade 7a including two sexually functional heterothallic hybrid species detected in natural ecosystems in Taiwan. *Persoonia* **38**: 100–135.

Jung T, Nechwatal J, Cooke DEL, Hartmann G, Blaschke M, *et al*. (2003) *Phytophthora pseudosyringae* sp. nov., a new species causing root and collar rot of deciduous tree species in Europe. *Mycological Research* **107**: 772–789.

Jung T, Orlikowski L, Henricot B, Campos P, Aday AG, *et al*. (2016) Widespread *Phytophthora* infestations in European nurseries put forest, semi-natural and horticultural ecosystems at high risk of *Phytophthora* diseases. *Forest Pathology* **46**: 134–163.

Jung T, Scanu B, Bakonyi J, Seress D, Kovács GM, *et al.* (2017c) *Nothophytophthora* gen. nov., a new sister genus of *Phytophthora* from natural and semi–natural ecosystems. *Persoonia* **39**: 143–174.

Jung T, Vettraino AM, Cech TL, Vannini A (2013) The impact of invasive *Phytophthora* species on European forests. In: *Phytophthora*: *a global perspective* (Lamour K, ed.): 146–158. Wallingford: CAB International.

Katoh K, Standley DM (2013) MAFFT multiple sequence alignment software version 7: improvements in performance and usability. *Molecular Biology and Evolution* **30**: 772–780.

Kremer A, Abbott AG, Carlson JE, Manos PS, Plomion C, *et al*. (2012) Genomics of *Fagaceae*. *Tree Genetics and Genomes* **8**: 583–610.

Kroon LPNM, Bakker FT, van den Bosch GBM, Bonants PJM, Flier WG (2004) Phylogenetic analysis of *Phytophthora* species based on mitochondrial and nuclear DNA sequences. *Fungal Genetics and Biology* **41**: 766–782.

Logan WB (2005) *Oak*: *the frame of civilization*. New York: W W Norton.

Man in 't Veld WA (2007) Gene flow analysis demonstrates that *Phytophthora fragariae* var. *rubi* constitutes a distinct species, *Phytophthora rubi* comb. nov. *Mycologia* **99**: 222–226

Manos PS, Stanford AM (2001) The biogeography of *Fagaceae*: tracking the Tertiary history of temperate and subtropical forests of the Northern Hemisphere. *International Journal of Plant Science* **162**: S77–S93.

Martin FN, Tooley PW (2003) Phylogenetic relationships among *Phytophthora* species inferred from sequence analysis of mitochondrially encoded cytochrome oxidase I and II genes. *Mycologia* **95**: 269–284.

Martin FN, Blair JE, Coffey MD (2014) A combined mitochondrial and nuclear multilocus phylogeny of the genus *Phytophthora*. *Fungal Genetics and Biology* **66**: 19–32.

Martìn-Garcìa J, Solla A, Corcobado T, Siasou E, Woodward S (2015) Influence of temperature on germination of *Quercus ilex* in *Phytophthora cinnamomi*, *P. gonapodyides*, *P. quercina* and *P. psychrophila* infested soils. *Forest Pathology* **45**: 215–223.

Nagy ZÁ, Bakonyi J, Érsek T (2003) Standard and Swedish variant types of the hybrid alder *Phytophthora* attacking alder in Hungary. *Pest Management Science* **59**: 484–492.

Oudemans P, Coffey MD (1991) Isozyme comparison within and among worldwide sources of three morphologically distinct species of *Phytophthora*. *Mycological Research* **95**: 19–30.

Paap T, Croeser L, White D, Aghighi S, Barber P, St. J. Hardy GE, Burgess TI (2017) *Phytophthora versiformis* sp. nov., a new species from Australia related to *P. quercina*. *Australasian Plant Pathology*: DOI 10.1007/s13313-017-0499-7.

Pánek M, Fér T, Mráček J, Tomšovský M (2016) Evolutionary relationships within the *Phytophthora cactorum* species complex in Europe. *Fungal Biology* **120**: 836-851.

Pérez-Sierra A, López-García C, León M, García-Jiménez J, Abad-Campos P, *et al*. (2013) Previously unrecorded low temperature *Phytophthora* species associated with *Quercus* decline in a Mediterranean forest in Eastern Spain. *Forest Pathology* **43**: 331–339.

Rahman MZ, Uematsu S, Kimishima E, Kanto T, Kusunoki M, *et al*. (2015) Two plant pathogenic species of *Phytophthora* associated

with stem blight of Easter lily and crown rot of lettuce in Japan. *Mycoscience* **56**: 419–433.

Rea AJ, Burgess TI, Hardy GEStJ, Stukely MJC, Jung T (2011) Two novel and potentially endemic species of *Phytophthora* associated with episodic dieback of kwongan vegetation in the south-west of Western Australia. *Plant Pathology* **60**: 1055–1068.

Robideau GP, de Cock AWAM, Coffey MD, Voglmayr H, Brouwer H, *et al*. (2011) DNA barcoding of oomycetes with cytochrome c oxidase subunit I (COI) and internal transcribed spacer (ITS). *Molecular Ecology Resources* **11**: 1002–1011.

Ronquist F, Heuelsenbeck JP (2003) MrBayes 3: Bayesian phylogenetic inference under mixed models. *Bioinformatics* **19**: 1572–1574.

Saavedra A, Hansen EM, Goheen DJ (2007) *Phytophthora cambivora* in Oregon and its pathogenicity to *Chrysolepis chrysophylla*. *Forest Pathology* **37**: 409–419.

Scanu B, Linaldeddu BT, Franceschini A (2010) First report of *Phytophthora pseudosyringae* associated with ink disease of *Castanea sativa* in Italy. *Plant Disease* **94**: 1068.

Scanu B, Hunter GC, Linaldeddu BT, Franceschini A, Maddau L, *et al.* (2014a) A taxonomic re-evaluation reveals that *Phytophthora cinnamomi* and *P. cinnamomi* var. *parvispora* are separate species. *Forest Pathology* **44**: 1–20.

Scanu B, Linaldeddu BT, Deidda A, Jung T (2015) Diversity of *Phytophthora* species from declining Mediterranean maquis vegetation, including two new species, *Phytophthora crassamura* and *P. ornamentata* sp. nov. *PLoS ONE* **10** (12): e0143234.

Scanu B, Linaldeddu BT, Franceschini A, Anselmi N, Vannini A, *et al*. (2013) Occurrence of *Phytophthora cinnamomi* in cork oak forests in Italy. *Forest Pathology* **43**: 340–343.

Scanu B, Linaldeddu BT, Peréz-Sierra A, Deidda A, Franceschini A (2014b) *Phytophthora ilicis* as a leaf and stem pathogen of *Ilex aquifolium* in Mediterranean islands. *Phytopathologia Mediterranea* **53**: 480–490.

Scanu B, Webber JF (2016) Dieback and mortality of *Nothofagus* in Britain: ecology, pathogenicity and sporulation potential of the causal agent *Phytophthora pseudosyringae*. *Plant Pathology* **65**: 26–36.

Schirone B, Radoglou K, Vessella F (2016) Conservation and restoration strategies to preserve the variability of cork oak *Quercus suber*–a Mediterranean forest species-under global warming. *Climate Research* **71** (2): 171–185.

Schwingle BW, Smith JA, Blanchette RA (2007) *Phytophthora* species associated with diseased woody ornamentals in Minnesota nurseries. *Plant Disease* **91**: 97–102.

Scott PM, Burgess TI, Barber PA, Shearer BL, Stukely MJC, Hardy GEStJ, Jung T (2009) *Phytophthora multivora* sp. nov., a new species recovered from declining *Eucalyptus*, *Banksia*, *Agonis* and other plant species in Western Australia. *Persoonia* **22**: 1–13.

Silvestro D, Michalak I (2012) raxmlGUI: a graphical front-end for RAxML. *Organisms, Diversity and Evolution* **12**: 335–337.

Simamora AV, Stukely MJC, Hardy GEStJ, Burgess TI (2015) *Phytophthora boodjera* sp. nov., a damping-off pathogen in production nurseries and from urban and natural landscapes, with an update on the status of *P. alticola*. *IMA Fungus* **6**: 319–335.

Staden R, Beal KF, Bonfield JK (2000) The Staden package 1998. *Methods in Molecular Biology* **132**: 115–130.

Stamatakis A (2014) RAxML version 8: a tool for phylogenetic analysis and post-analysis of large phylogenies. *Bioinformatics* **30**: 1312–1313.

Tamura K, Stecher G, Peterson D, Filipski A, Kumar S (2013) MEGA6: Molecular Evolutionary Genetics Analysis Version 6.0. *Molecular Biology and Evolution* **30**: 2725–2729.

Tang QH, Gao F, Li GY, Wang H, Zheng XB, Wang YC (2010) First report of root rot caused by *Phytophthora sansomeana* on soybean in China. *Plant Disease* **94**: 378.

Weir BS, Paderes EP, Anand N, Uchida JY, Pennycook SR, Bellgard SE, Beever RE (2015) A taxonomic revision of *Phytophthora* Clade 5 including two new species, *Phytophthora agathidicida* and *P. cocois*. *Phytotaxa* **205**: 21–38.

White TJ, Bruns T, Lee S, Taylor J (1990) Amplification and direct sequencing of fungal ribosomal RNA genes for phylogenetics. In: *PCR Protocols*: *a guide to methods and applications* (Innis MA, Gelfand DH, Sninsky JJ, White TJ, eds): 315–322. San Diego: Academic Press.

Yang X, Copes WE, Hong C (2014) Two novel species representing a new clade and cluster of *Phytophthora*. *Fungal Biology* **118**: 72–82.